CHAPTER 2

BACKGROUND AND LITERATURE REVIEW

This chapter focuses on the background of piezoelectricity, relationships between piezoelectric and dielectric properties, electromechanical coupling coefficients, thermal expansion, acoustic impedance, background of piezoelectric ceramic and modified barium titanate ceramic, portland cement (PC), composite materials and the review of literatures related to piezoelectric-cement based composites with 0-3, 1-3 and 2-2 connectivity type are given.

2.1 Piezoelectricity

A piezoelectric material has the unique ability to interchange electrical energy and mechanical strain energy or force. Due to this characteristic of the material, it has been found to be very effective for use in dynamic applications involving vibration suppression, mechanical impact and sensing. However piezoelectric materials have been used in numerous other applications including sonar application, audio buzzers, air ultrasonic transducers, sensor, actuator, energy harvesting and piezoelectric ceramic ignition systems [23-29].

2.1.1 History and basis for piezoelectricity Theory

Piezoelectricity was discovered in 1880 by French physicists Jacques and Pierre Curie. The first demonstration of the piezoelectric effect was discovered that some crystalline materials, when compressed, produced a voltage proportional to the

applied pressure and that when an electric field is applied across the material, there is corresponding change of shape. The word piezoelectricity means electricity resulting from pressure. The name “piezo” from a Greek word meaning to press and electricity is the end product [24]. So the piezoelectricity is understood as the generation of electricity as a result of a mechanical pressure. Piezoelectric theory is defined by Cady [25], “electric polarization produced by mechanical strain in crystals belonging to certain classes, the polarization being proportional to the strain and changing sign with it.”

The Piezoelectric materials have the piezoelectric effect and the piezoelectric effect is a reversible process in that materials exhibiting the direct piezoelectric effect (the internal generation of electrical charge resulting from an applied mechanical force) also exhibit the reverse piezoelectric effect (the internal generation of a mechanical strain resulting from an applied electrical field). Fundamental research has shown that piezoelectricity is based on a property of the elementary unit cell of the crystalline structure of the material, the essential condition being that the crystal unit cell should have no center of symmetry [26]. Not every dielectric can be a ferroelectric. Crystals can be classified into 32 point groups (Fig. 2.1) according to their crystallographic symmetry, and these point groups can be divided largely into two classes, one with a center of symmetry and the other without. 11 are centrosymmetric and consequently cannot exhibit polar properties. There are 21 point groups which do not have a center of symmetry. In crystals belonging 20 of these point groups, positive and negative charges appear on surfaces when stresses are applied. These materials are known as piezoelectrics and 10 have unique polar axes. These classes are called polar crystals because they are spontaneously polarized and

exhibit pyroelectricity. This polarization also changes with temperature hence the term pyroelectricity but ferroelectric crystals are only those crystals for which the spontaneous polarization can be reversed by applying an electric field [26-28].

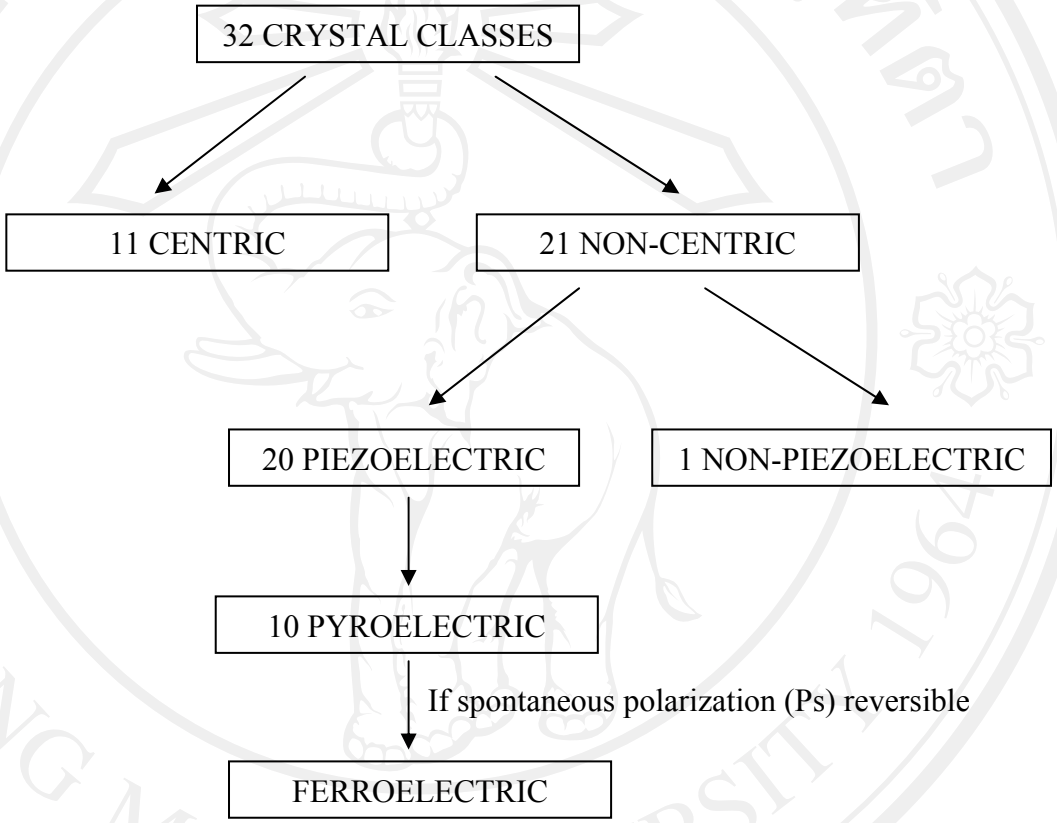

Fig. 2.1 Classification of the 32 crystallographic crystal classes [26].

2.1.2 Poling

Because a ceramic is composed of a large number of randomly oriented crystallites and the possibility of altering the direction of the polarization in the crystallites of a ferroelectric ceramic (a process called 'poling') makes it capable of piezoelectric [28]. The poling process is the critical element in being able to utilize

piezoelectric effect in a ferroelectric ceramic. Without poling, the ceramic is inactive, even though each one of the individual crystallites itself is piezoelectric. Before poling, ferroelectric ceramics do not possess any piezoelectric properties owing to the random orientations of ferroelectric domains [29]. During poling, a d.c. voltage for a sufficient time is applied on the ferroelectric ceramic sample to force the domain reorientation (or dipole rearrangement) and the material is said to be "poled". When the electric field is removed and a remanent polarization and a remanent strain are maintained in the sample cause to the sample exhibits piezoelectricity. A simple illustration of the poling process is shown in Fig. 2.2. With poling, it is important that appropriate poling field strength, time and usually at a temperature slightly below the Curie point be chosen [24, 30].

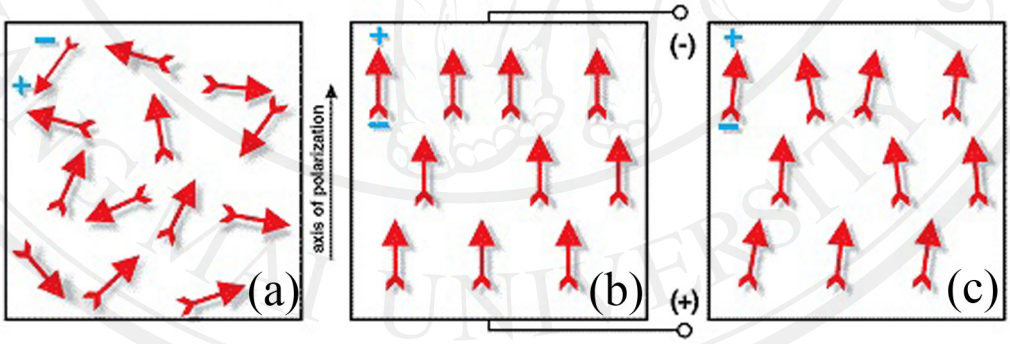

Fig. 2.2 Polarizing (poling) a piezoelectric ceramic; (a) random orientation of polar domains prior to polarization, (b) polarization in DC electric field and (c) after polarization [24].

A poled piezoelectric ceramic, will generate an electric field or current if subjected to physical stress and this property is referred to as the "direct piezoelectric effect". The same effect can also be observed in reverse, where an imposed electric

field on the crystal will put stress on its structure and this property is referred to as the "converse piezoelectric effect". The piezoelectric effect the basis upon which the piezoelectric materials are used as sensors and actuators applications [31].

2.2 Relationship between *g*, *ε* and *d* coefficients

As mentioned previously, two piezoelectric effects are defined as a change in electric polarization with a change in applied stress. This property is referred to as the direct piezoelectric effect (designated as a generator). The converse piezoelectric effect (designated as a motor) is the change of strain or stress in a material due to an applied electric field [24]. Both of these effects are shown in Fig. 2.3.

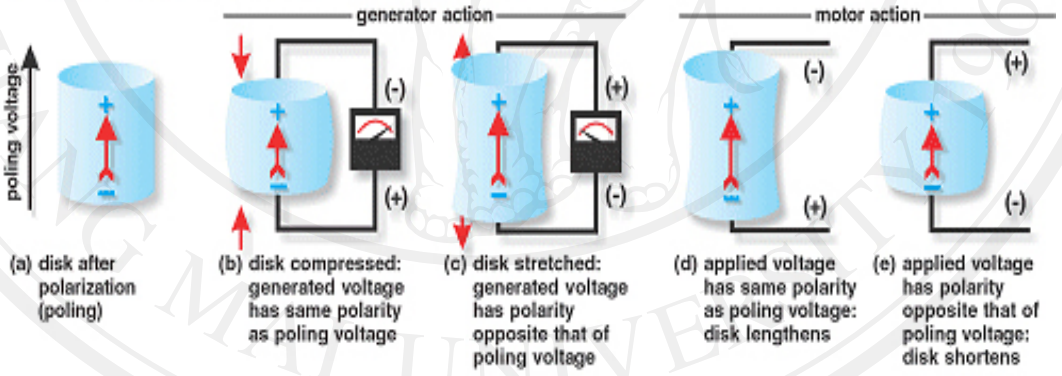

Fig. 2.3 Generator and motor actions of a piezoelectric element [29].

The piezoelectric *d* coefficient is a measure of the charge density per unit stress or the strain per unit field. Piezoelectric coefficients (d_{ik}) with double subscripts link electrical and mechanical quantities. The first subscript gives the direction of the electrical field associated with the voltage applied or the charge or the voltage produced. The second subscript gives the direction of mechanical stress or the strain

[29]. For d_{33} indicates the polarization generated in the 3 direction when the stress is applied in the 3 direction. The d coefficients are numerically equal in both equations and usually expressed as $\times 10^{-12}$ C/N for the direct effect and $\times 10^{-12}$ m/V for the converse effect. The piezoelectric voltage coefficient; g means the sensitivity of a receiving voltage, open-circuit g coefficients are also used to evaluate piezoelectric ceramics for their ability to generate large amounts of voltage per unit of input stress. The relationship between g, ε and d coefficients [23, 26];

$$g = \frac{d}{\varepsilon \varepsilon_0} \tag{2.1}$$

For the most applications of ferroelectric materials the dielectric properties are important practical parameter, and studies of dielectric properties provide a great deal of information for understanding the basic properties of materials. The relative dielectric constant can be calculated using the following formulas:

$$\varepsilon = \frac{Ct}{\varepsilon_0 A} \tag{2.2}$$

Where ε is the relative dielectric constant, C is the sample capacitance, t is the thickness, ε_0 is the permittivity of free space constant (8.854×10^{-12} F/m), and A is the electrode area. Therefore, the low ε_r and high d coefficients which corresponds to high g coefficients as shown in the following Eq. (2.1). For the lower ε values and high g coefficients material are usually ferroelectrically hard materials that do not switch their polarization suddenly [26, 32].

2.3 Electromechanical coupling coefficients

Sometimes also referred as electromechanical coupling coefficients, these describe the conversion of energy by the ceramic element from electrical to mechanical form or vice-versa [29].

$$K = \frac{\text{Mechanical Energy stored}}{\text{Electrical Energy applied}} \quad (2.3)$$

$$K = \frac{\text{Electrical Energy applied}}{\text{Mechanical Energy stored}} \quad (2.4)$$

The electrical properties of a piezoelectric vibrator are dependent on the many properties such as piezoelectric, elastic, and dielectric constants of the vibrator materials. For K_t is thickness electromechanical coupling coefficient. The electromechanical coupling coefficient (K_t) was then calculated from the electric impedance graph plotted against the frequency and using the following formula [33]:

$$K_t^2 = \frac{\pi}{2}\frac{f_s}{f_p}\tan\left(\frac{\pi}{2}\frac{f_p - f_s}{f_p}\right) \quad (2.5)$$

where f_s and f_p are the series frequency and the parallel resonance frequency, respectively, and K_t can be approximated as follows:

$$K_t^2 = \frac{\pi}{2}\frac{f_m}{f_n}\tan\left(\frac{\pi}{2}\frac{f_n - f_m}{f_n}\right) \quad (2.6)$$

where f_m and f_n are the frequency at the minimum and maximum electric impedance respectively, which can be approximately replaced by frequency f_m and f_n, that is, $f_s \approx f_m, f_p \approx f_n$.

2.4 Thermal Expansion

Thermal expansion is defined as the tendency of matter to change in volume in response to a change in temperature. When change in temperature, the solid materials is expanded when heating and contracted upon cooled. The change in length in response to a change in temperature for a solid material can be expressed as [34-35]:

$$\left(l_f - l_0\right)/l_0 = \alpha_1\left(T_f - T_0\right) \tag{2.7}$$

$$\Delta l/l_0 = \alpha_1\left(\Delta T\right) \tag{2.8}$$

Where l_0 and l_f represent, respectively, the original and final lengths with the temperature change from T_0 to T_f. The parameter α_1 (CTE or α) is called the linear coefficient of thermal expansion; CTE and it is a material property that is indicative of the extent to which a material expands upon heating, and has units of reciprocal temperature [$(^oC)^{-1}$, $(^oK)^{-1}$ or $(^oF)^{-1}$]. Of course, heating or cooling affects all the dimensions of a body, with a result change in volume. Volume changes with temperature may be computed from:

$$\Delta V/V_0 = \alpha_V \Delta T \tag{2.9}$$

where ΔV and V_0 are the volume change and original volume, respectively, and α_V represents the volume coefficient of thermal expansion. In many materials, the value of α_V is anisotropic; that is, it depends on the crystallographic direction along which it is measured. For materials in which the thermal expansion is isotropic, α_V is approximately $3\alpha_1$ [36].

Thermal expansion is reflected by an increase in the average distance between the atoms. From Fig. 2.4(a), the curve is in the form of a potential energy trough, and the equilibrium interatomic spacing at 0 K, r_0, corresponds to the trough minimum.

Heating to successively higher temperatures (T_1, T_2, T_3, etc.) raises the vibrational energy from E_1 to E_2 to E_3, and so on. The average vibrational amplitude of an atom corresponds to the trough width at each temperature, and the average interatomic distance is represented by the mean position, which increases with temperature from r_0 to r_1 to r_2, and so on [35-36].

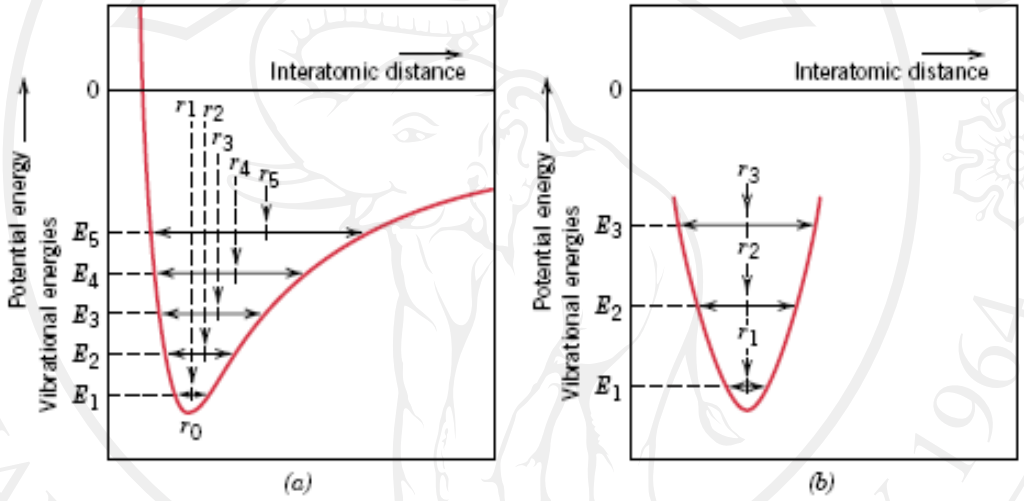

Fig. 2.4 (a) Plot of potential energy versus interatomic distance, demonstrating the increase in interatomic separation with rising temperature. With heating, the interatomic separation increases from r_0 to r_1 to r_2, and so on. (b) For a symmetric potential energy-versus-interatomic distance curve, there is no increase in interatomic separation with rising temperature (i.e., $r_1 = r_2 = r_3$) [36].

For a symmetric potential energy-versus-interatomic distance curve, there is no increase in interatomic separation with rising temperature (i.e., $r_1 = r_2 = r_3$) is shown in Fig. 2.4(b). Thermal expansion is really due to the asymmetric curvature of this potential energy trough, rather than the increased atomic vibrational amplitudes with

rising temperature. If the potential energy curve were symmetric, there would be no net change in interatomic separation and, consequently, no thermal expansion. Each class of materials such as metals, ceramics, and polymers, the greater the atomic bonding energy, the deeper and more narrow this potential energy trough cause to a smaller value of α_l when the increase in interatomic separation with a given rise in temperature will be lower [36].

For many ceramic materials are found relatively strong interatomic bonding forces as reflected in comparatively low coefficients of thermal expansion (values typically range between about 0.5×10^{-6} and 15×10^{-6} $(^{o}C)^{-1}$) [36]. The linear coefficient of thermal expansion is isotropic for noncrystalline ceramics and also those having cubic crystal structures. Otherwise, it is anisotropic; and some ceramic materials, upon heating, contract in some crystallographic directions while expanding in others. Ceramic materials that are to be subjected to temperature changes must have relatively low coefficients of thermal expansion, and in addition, isotropic. Moreover, the ceramic is brittle materials and it may experience fracture as a consequence of nonuniform dimensional changes in what is termed thermal shock [34-36]. For concrete, the coefficient of thermal expansion will be a variable quantity depending on the mix design and the type of aggregate used and the α_l values of concrete is range between about $7.4\text{-}13 \times 10^{-6}$ $(^{o}C)^{-1}$ [37].

2.5 Acoustic Impedance

The acoustic impedance of a material is its most fundamental acoustic property. Impedance is defined as the ratio of the pressure to the volume displacement at a given surface in a sound-transmitting medium, is usually a frequency-dependent

complex number. Because the acoustic impedance of a material determines the acoustic response of the surrounding environs, careful impedance measurements are required to produce accurate system models. Acoustic enclosure designers can then use these models to select suitable materials for wall, floor, and ceiling coverings. Sound travels through materials under the influence of sound pressure. Because molecules or atoms of a solid are bound elastically to one another, the excess pressure results in a wave propagating through the solid [38-39].

Mathematically, it is the sound pressure p divided by the particle velocity v and the surface area S, through which an acoustic wave of frequency f propagates. If the impedance is calculated for a range of excitation frequencies the result is an impedance curve. Planar, single-frequency traveling waves have acoustic impedances equal to the characteristic impedance divided by the surface area, where the characteristic impedance is the product of longitudinal wave velocity and density of the medium. Acoustic impedance can be expressed in either its constituent units (pressure per velocity per area) or in rayls per square meter. The acoustic impedance (Z) of a material is defined as the product of its density (ρ) and acoustic velocity (V); $Z = \rho V$. Acoustic impedance is important in the determination of acoustic transmission and reflection at the boundary of two materials having different acoustic impedances, the design of ultrasonic transducers and assessing absorption of sound in a medium. The acoustic impedance for any material was obtained by multiplying the density (ρ) with the velocity (V) and the acoustic impedance also shows how a change in the impedance affects the amount of acoustic energy that is reflected and transmitted [3, 38].

2.6 Background of piezoelectric ceramic and modified barium titanate ceramic

In the past, innovations in sensors, actuators and ultrasonic transducers have been the driving force for new developments of piezoelectric ceramics [40]. A major breakthrough came with the discovery of PZT and $BaTiO_3$ in the 1950s and the family of these materials exhibited very high dielectric and piezoelectric properties show in Fig. 2.5.

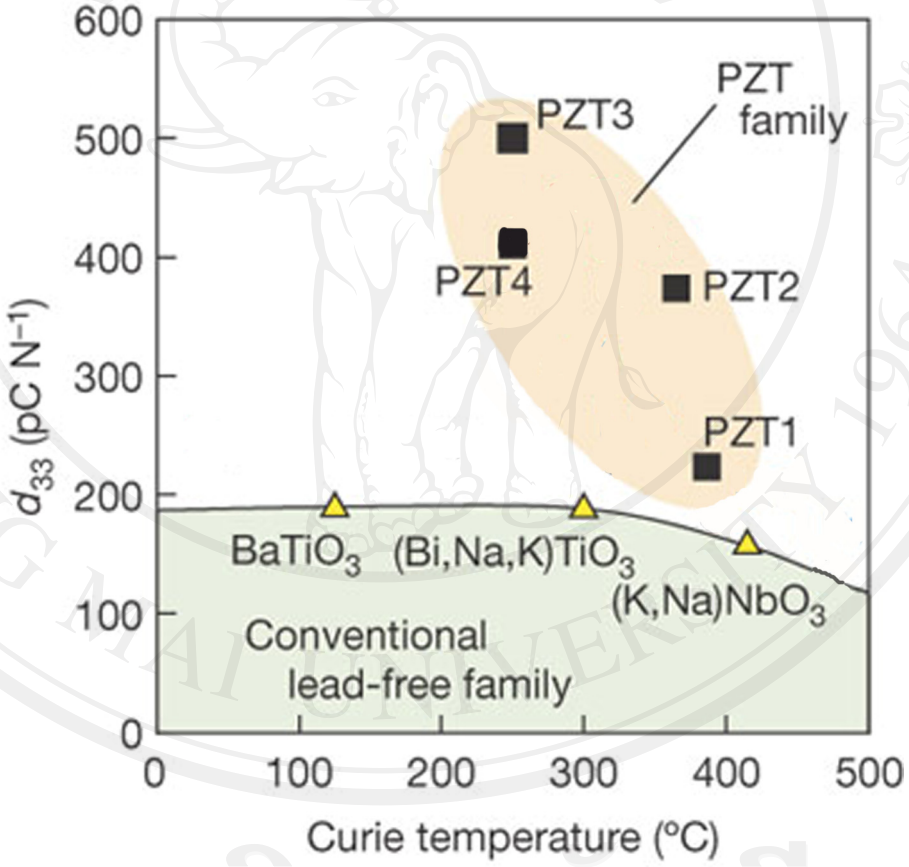

Fig. 2.5 Comparison of the d_{33} value for the piezoelectric ceramic [41].

To date, PZT is one of the most widely exploited and extensively used piezoelectric materials, having secured a permanent place in the field of material

science and engineering. They are widely used as sensor and actuator devices, multilayered capacitors, as hydrophones, etc. with an estimated market of tens of billions of dollars worldwide. However, lead oxide, which is a component of PZT, is highly toxic and its toxicity is further enhanced due to its volatilization at high temperature particularly during calcination and sintering causing environmental pollution [20].

Ferroelectric materials such as barium titanate $BaTiO_3$ appear to be the most important among the variety of ceramic materials. The $BaTiO_3$ is one of the most widely studied lead-free piezoelectric materials. $BaTiO_3$ has been a widely studied ceramic system due to its ferroelectric and electromechanical features and has been extensively modified (doped) with the small amounts of variety additives that make them more attractive for any specific application. $BaTiO_3$-based ceramics find applications in many modern disciplines such as automatics, micromanipulation, measuring techniques, medical diagnostics (i.e. multilayer capacitors, actuators, sensor, transducers, and ultrasound imaging) [15]. It has been well documented that small amounts of impurity ions can dramatically modify the properties of BT materials in general [16]. It is well known that the phase transition temperature in $BaTiO_3$ can be altered by doping with either A or/and B site (ABO_3) substitutions e.g., the addition of calcium (Ca^{2+}), Strontium (Sr^{2+}) into barium (Ba^{2+}) site or zirconium (Zr^{4+}), tin (Sn^{4+}) into titanium (Ti^{4+}) B-site in barium titanate [42-47].

Table 2.1 Summary of the dielectric properties and piezoelectric coefficient of $BaTiO_3$-based ceramics.

Properties	BT 23%Ca [43]	BT 2.5%Sn [44]	BT 4%KN** [45]	BT 5%Zr [13, 18]	BT 40%Sr [46]
Dielectric constant	≈950	1238*	-	1227[14]	≈3300
Dielectric loss	-	0.02	-	0.03[14]	≈0.01
d_{33} (pC/N)	≈150	111	215	224[14], 236[18]	-

*The dielectric constant was measurement at frequency 100 kHz.

**For BT 4%KN is $BaTi_{1-x}(KNb)_xO_3$

The summary of the dielectric properties and piezoelectric coefficient of $BaTiO_3$-based ceramics is given in Table 2.1. However, not all conditions were the same and that direct comparison is not possible. Barium zirconate titanate ($BaTi_{1-x}Zr_xO_3$; BZT) is obtained by substituting ions at B site of $BaTiO_3$ with Zr ions. The BZT ceramics were extensively investigated and show promising piezoelectric/electrostrictive properties [17]. Thus, BZT ceramic presents a great interest both for applications in the field of environmental protection and this material is of interest as a candidate to replace lead-based ceramic [18-19].

BZT ceramic

In the mid-1950s, Brajer [48] and Kulscar [49] showed that, as the zirconium content increases, the orthorhombic-tetragonal phase transition increases and the

tetragonal cubic phase transition decreases. The first dependence of the phase transition temperatures on the zirconium content was first shown by Kell and Hellicar [50]. Verbiskaja *et at.* [51] reported a direct orthorhombic-cubic phase transition for zirconium contents of >15%. Other authors have assumed the coexistence of both the orthorhombic and tetragonal phases within a small temperature interval at the Curie point (T_C). The latter has been confirmed by detailed investigation. In addition, a broadening of this temperature range of coexisting crystal structures with to decreasing zirconium content has been observed, with a subsequent separation of the structural phases with further decreases in the amount of zirconium [52].

Hennings *et al.* [53] gave an explanation of the temperature characteristics of the permittivity. Calorimetric measurements at the T_C value showed a clear decrease in the latent heat, disappearing at a zirconium content of ≈ 10%, and suggesting a change from first order to second-order transitions at low zirconium contents. Further increases in the amount of zirconium results in a stimulated broadening of the (T_C) curve. This phenomenon is due to the increased sensitivity of the ceramic, relative to local structural transitions in the vicinity of T_C, which leads to a distribution of Curie maxima and, thus, a broad, resulting envelope. This phenomenon is called a diffuse phase transition (DPT) and appears at zirconium contents of >13%, according to Hennings *et al.* [53].

The phase diagram for $Ba(Ti_{1-x}Zr_x)O_3$ ceramics with $0<x<0.3$ are presented in Fig. 2.6. Compared with the three phase transitions in pure BT at T_C = 120 ºC, T_2 = 0 ºC, and T_3 = -90 ºC, the paraelectric to ferroelectric phase transition T_C for $Ba(Ti_{1-x}Zr_x)O_3$ crystals is shifted to lower temperatures with increasing Zr concentration. It is reported that an increase in the Zr content induces a reduction in the average grain

size, decreases the dielectric constant, and maintains a leakage current low and stable. This is possible because the Zr^{4+} ion has larger ionic size (0.087 nm) than Ti^{4+} (0.074 nm) [54]. Investigation has shown that the phase transition behavior of BZT materials can be changed from a normal phase transition to diffusive and further become a relaxor phase transition.

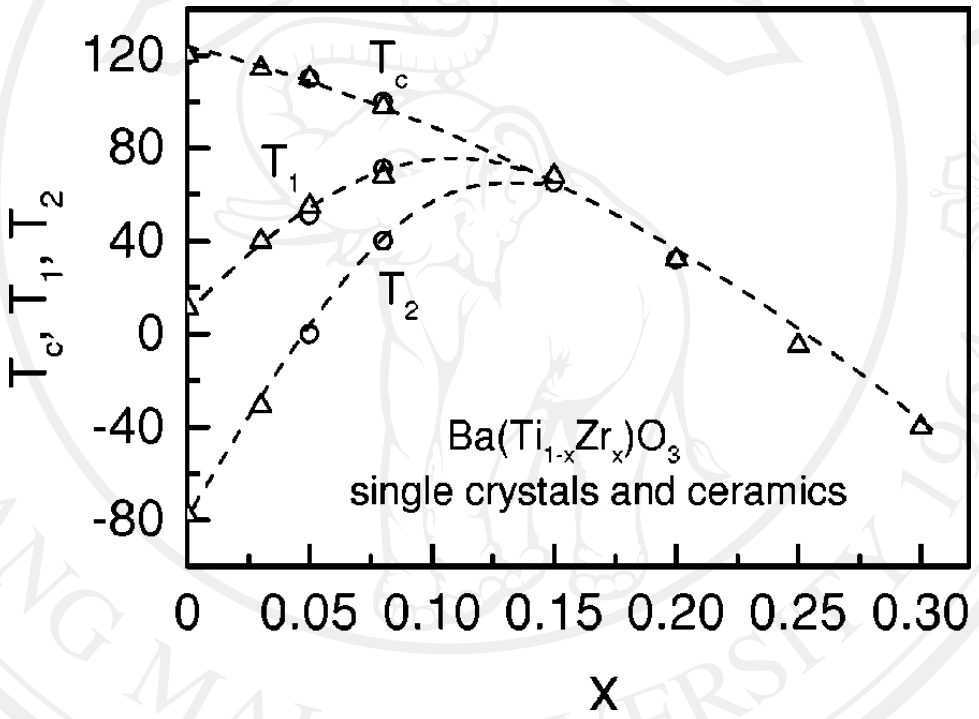

Fig. 2.6 Phase diagram for $Ba(Ti_{1-x}Zr_x)O_3$ ceramics with $0<x<0.3$. (For various compositions, data were taken at 1 kHz. Symbols are experimental data: up-triangles: data for ceramics; open circles: single crystal data; Dash curves: guide to the eyes) [18].

Yu *et al.* [18] reported piezoelectric and strain properties of $Ba(Ti_{1-x}Zr_x)O_3$ ceramics. $Ba(Ti_{1-x}Zr_x)O_3$ ceramics were prepared via methods of the solid state reaction in 2002. Zr-doped $BaTiO_3$ (BZT) ceramics with 5% Zr content showed fairly

satisfactory piezoelectric response, with the piezoelectric constant value of 236 pC/N at room temperature in Table 2.2 [18].

Table 2.2 Dielectric constant (ε), density, electromechanical coupling coefficients (K), elastic compliance (s), and piezoelectric strain coefficients (d) of $Ba(Ti_{1-x}Zr_x)O_3$ ceramics [18].

	x = 0.03	**x = 0.05**	**x = 0.08**
ε_{33}^{D}	1900	1700	1100
ε_{33}^{E}	1800	1600	900
Density (kg/m^3)	5800	5800	5300
K_{31} (%)	22.1	17.0	-
K_{33} (%)	42.9	56.5	41.4
s_{11}^{E} (10^{-12} m^2/N)	8.75	8.45	-
s_{11}^{D} (10^{-12} m^2/N)	8.41	8.25	-
s_{33}^{E} (10^{-12} m^2/N)	9.95	10.4	10.1
s_{11}^{D} (10^{-12} m^2/N)	8.42	7.34	8.63
d_{31} (pC/N)	84	61	-
d_{33} (pC/N)	174	236	130

For the $Ba(Ti_{0.95}Zr_{0.05})O_3$ is normal ferroelectric materials. In 2010, Li *et al.* [19] studied the dielectric and piezoelectric properties of $Ba(Ti_{1-x}Zr_x)O_3$ lead-free ceramics. Lead-free $Ba(Ti_{1-x}Zr_x)O_3$ (x =0.02-0.2) ceramics prepared by solid-state reaction were systemically investigated. The ceramics at x =0.05 exhibited excellent

piezoelectric properties of high d_{33} = 208 pC/N, k_p = 31.5% and Q_m = 500. The piezoelectric properties of BZT ceramic are shown in Fig. 2.7.

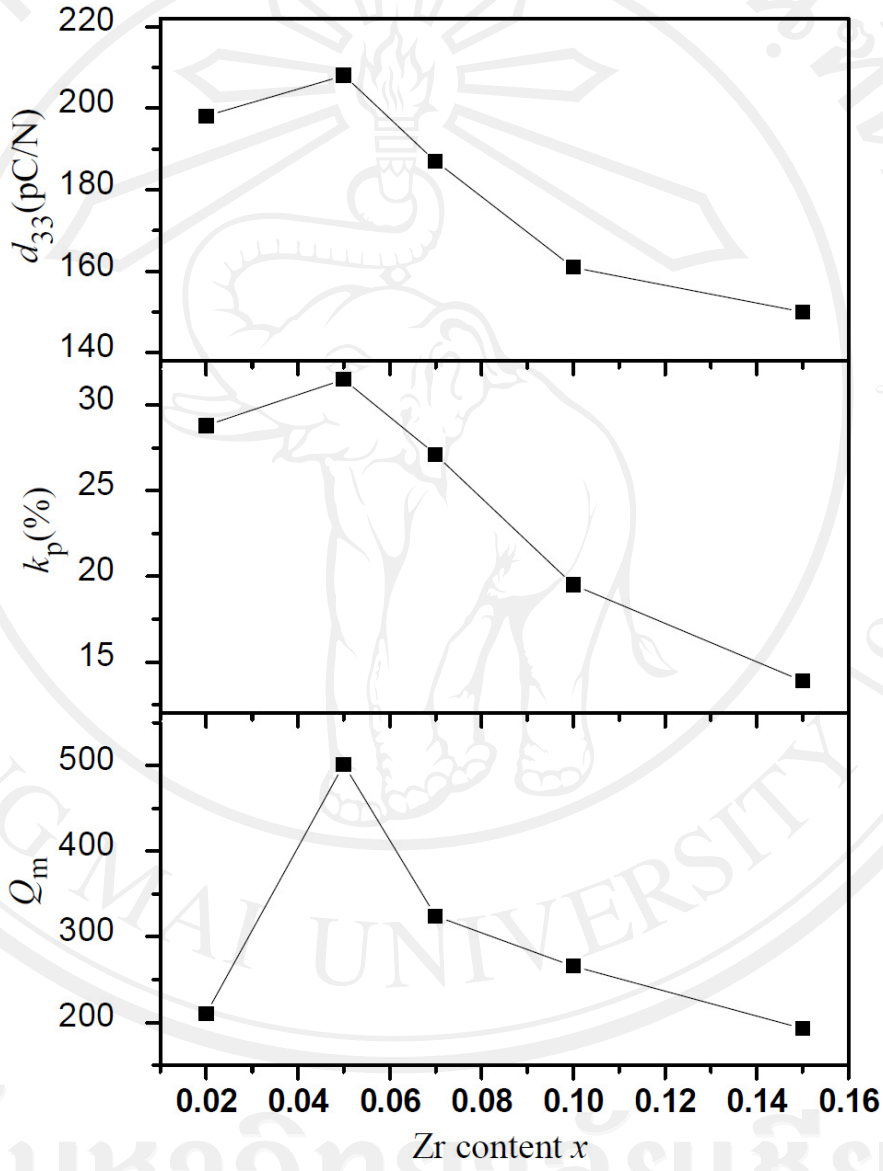

Fig. 2.7 Piezoelectric constant d_{33}, planar electromechanical coefficient k_p and mechanical quality factor Q_m of the $Ba(Zr_xTi_{1-x})O_3$ ceramics as a function of x [19].

2.7 Portland cement

2.7.1 Definition of Portland cement

Portland cement is the most commonly used type of cement (often referred to as OPC, from Ordinary Portland Cement). Portland cement is a basic ingredient of concrete and the most common use for Portland cement is in the production of concrete. In additional, ASTM C 150 defines Portland cement as a hydraulic cement produced by pulverizing clinkers consisting essentially of hydraulic calcium silicates, and a small amount of one or more forms of calcium sulfate as an interground addition. Clinkers are 5- to 25-mm-diameter nodules of a sintered material that is produced when a raw mixture of predetermined composition is heated to high temperatures [55].

2.7.2 Composition of Portland cement

Cement manufacturing operations require raw materials of sufficient purity with uniform composition for producing high quality Portland cement. The compounds that form Portland cement are the result of a partial solid state reaction involving mainly lime on the one hand and silica, alumina and ferric oxide on the other [56]. The most common source of calcium oxide is limestone (calcium carbonate) and although other forms of calcium carbonate such as chalk, shell deposits, and calcareous muds, are used. In principle, the manufacture of portland cement is simple. It is made from abundant raw materials. An intimate mixture raw materials, usually limestone and clay together is heated in kiln at very high temperatures ranging from 1,400 to 1,600 ºC, which is the temperature range in which these materials interact chemically to form the calcium silicates [37].

Table 2.3 Typical oxide and compound compositions of Portland cements [57].

		Abbreviation	Ordinary %
Oxides	CaO	C	63.1
	SiO_2	S	20.6
	Al_2O_3	A	6.3
	Fe_2O_3	F	3.6
	MgO	M	0.8
	Na_2O	N	0.3
	K_2O	K	0.6
	SO_3	S	2.6
	TiO_2	T	0.4
Compounds	$3CaO \cdot SiO_2$	C_3S	39
	$2CaO \cdot SiO_2$	βC_2S	30
	$3CaO \cdot Al_2O_3$	C_3A	11
	$4CaO \cdot Al_2O_3 \cdot Fe_2O_3$	C_4AF	11
	Free Lime	Free Lime	1.7

The oxide and potential compound compositions of typical Portland cements are given in Table 2.3. For using these oxide analyses and the compound stoichiometries, it is a sample matter to calculate a compound composition. This is known as the Bogue calculation [57-58]. Moreover, the four major compounds in Portland cements have compositions approximating to tricalcium silicate C_3S, dicalcium silicate C_2S, tricalcium aluminate C_3A and tetracalcium alumino ferrite C_4AF. The presence of an excess of uncombined or free lime must be avoided in cement clinker, since it undergoes an increasing in volume during hydration, so weakening the hardened paste. Other minor components to be found in cement clinker in small quantities include magnesium oxide and the alkaline oxides K_2O and Na_2O. These oxides affect

the idealized compound structure and hydraulic properties of cements to an extent which has yet to be determined [37].

2.7.3 The hydration of Portland cement

When Portland cement mixed with water to form pastes, the various hydration products that are formed in hydrated cement pastes have quite diverse properties, and the behavior of each compound will contribute to the overall behavior of the paste. These are reviewed in the following section.

Calcium Silicates

The principal hydration product is a calcium silicate hydrate. The hydration of tricalcium silicate (C_3S) and beta dicalcium silicate (βC_2S) in portland cement produces a family of calcium silicate hydrates which are structurally similar but vary widely in calcium/silica ratio and the content of chemically combined water. Since the structure determines the properties, the compositional differences among the calcium silicate hydrates have a little effect on their physical characteristics.

Tricalcium silicate (C_3S) has all the attributes of Portland cement. When finely ground and mixed with water, it hydrates quickly and crystals of calcium hydroxide $Ca(OH)_2$ are rapidly precipitated. Around the original grains, a gelatinous hydrated calcium silicate is formed which, being impermeable, slows down further hydration considerably. Hydrated C_3S sets or stiffens within a few hours and gains strength very rapidly, attaining the greater part of its strength within one month [55].

Beta dicalcium silicate (βC_2S) the hydraulic form of C_2S, exhibits no definite setting time, but does stiffen slowly over a period of some days. It produces little

strength for about fourteen days, but after one year its strength is equal to that of C_3S. The greater reactivity of C_3S can be attributed to the more open structure of the crystal lattice of C_3S compared with the denser packing of the ion in βC_2S [59].

For C_2S hydrates in a similar manner, but is much slower because it is a less reactive compound than C_3S. The amount of heat liberated by hydration of C_2S is also lower than it is with C_3S, and thus its calorimetric curve is not easy to measure experimentally [37].

Tricalcium aluminate C_3A, in portland cement, the hydration of C_3A involves reaction with sulfate ions that are supplied by the dissolution of gypsum. The tricalcium aluminate is very rapidly with water and the paste sets almost instantly with the evolution of so much heat that it may dry out. The addition of 3-4% to cement clinker, which corresponds to 25-50% of the C_3A content, produces a normal setting time. Hydrated C_3A produces little strength and has a low resistance to sulphate attack [37].

The calcium sulfoaluminate hydrate, whose correct name is 6-calcium aluminate trisulfate-32-hydrate, is commonly called “ettringite,” which is the name given to a naturally occurring mineral of the same composition. Ettringite is a stable hydration product only while there is ample supply of sulfate available. If the sulfate is all consumed before the C_3A has completely hydrated, then ettringite transforms to another calcium sulfoaluminate hydrate containing less sulfate. This second product is called tetracalcium alumuinate monosulfate-12-hydrate, or simply mono sulfoaluminate. Monosulfoaluminate may sometimes form before ettringite if hydrating C_3A consumes the sulfate ions faster than they can be supplied by dissolution of the gypsum in the mix water. The formation of monosulfoaluminate

occurs because in most cements there is not sufficient gypsum necessary to form ettringite from all the available aluminate ions [37].

Tetracalcium aluminoferrite C_4AF, or the ferrite phase, reacts quickly with water, but less rapidly than C_3A, and develops little strength. The C_4AF forms similar hydration products to C_3A, with or without gypsum. The reactions are slower and involve less heat; C_4AF seldom hydrates rapidly enough to cause flash set, and gypsum retards C_4AF hydration even more drastically than it does C_3A [37, 56].

The rate of hydration during the first few days is in the approximate order $C_3A>C_3S>C_4AF>C_2S$. It must be remembered, however, that no two preparations of any of these compounds will hydrate at exactly the same rate because their reactivities will be affected by differences in fineness and the rate of cooling of the clinker. There will be additional factors, such as the presence of impurities and the presence of the other cement compounds. For example, alite and belite hydrate faster than do pure C_3S and C_2S because of the impurity atoms contained in the structure. The hydration of C_3A and the ferrite phase will also be affected by impurity oxides [37, 56].

The strength developed by Portland cement compounds are shown in Fig. 2.8. It is the formation of CSH which gives the cement its strength. The laths and needles formed due to the reactions of C_3A and C_4AF result in the initial set of the cement, but these do not contribute significantly to the long-term strength. C_3S form CSH much more rapidly than C_2S; therefore cement with a higher proportion of C_3S will develop strength more rapidly than cements will less C_3S. While it is agree that the formation CSH gel are the major factors which contribute to the strength of cement, the role of the CH platelets is still uncertain. The rates of hydration are important; C_3A, C_4AF and C_3S all hydrate rapidly, but C_3S is responsible for the major part of the early

strength developed. C_2S hydrates more slowly, and it is this that gives the cement its increase in strength over the long term. It is the hydration of C_3S and C_3A that is responsible for most of the heat evolved in the cement in the first 48 hours. Therefore if this heat evolution is to be limited, C_3A and C_3S should be reduced (this involves a corresponding increase in C_2S, which results in a reduction in early strength but not in the ultimate strength of the cement) [57-59].

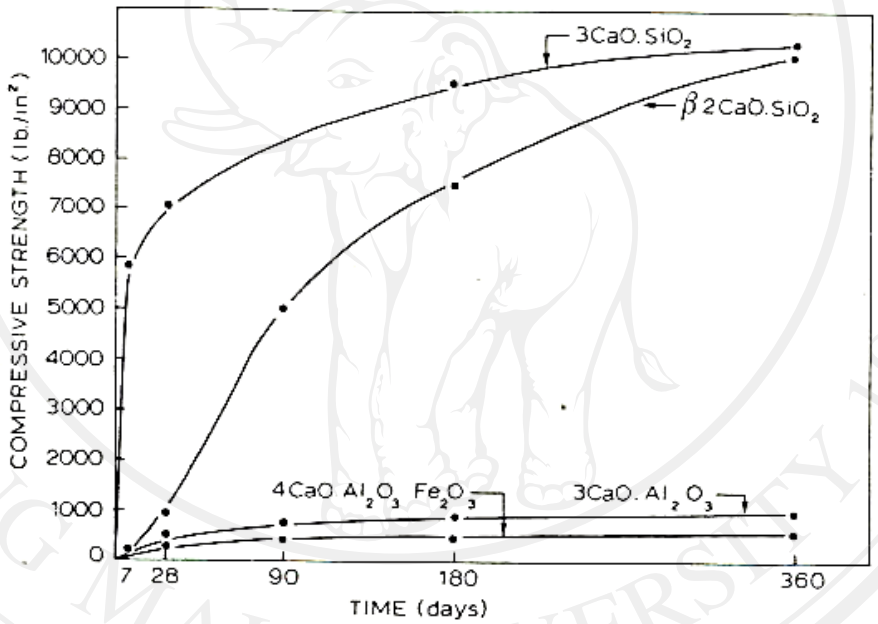

Fig. 2.8 The strength developed by Portland cement compounds [58].

2.7.4 Effect of temperature on the cement paste

Hydrated cement paste is composed of four major compounds: tricalcium silicate (C_3S), dicalcium silicate (C_2S), tricalcium aluminate (C_3A) and tetracalcium aluminoferrite (C_4AF). The most important products of the hydration reactions are the calcium silicate hydrate (C-S-H) and the portlandite, also called calcium hydroxyde, (CH). Different authors have described the reactions that occur with an increase of

temperature in cement paste and concrete. The 30-105 ºC: the evaporable water and a part of the bound water escapes. It is generally considered that the evaporable water is completely eliminated at 120 ºC. The 180-300 ºC: the loss of bound water from the decomposition of the C-S-H [60].

The sensitivity of C-S-H gel to achieved temperature level is evident from average C-S-H composition at 25 ºC $C_{1.88}SH_{1.52}$ and at 100 ºC $C_{2.04}SH_{0.98}$. These results clearly show the influence of temperature on the C/S and H/S ratios of C-S-H gel. Thermal treatment reduces the amount of bound water and increases [61]. The high temperature tends to change the mechanism of ettringite formation; a marked reduction in stability of ettringite between 60 and 80 ◦C is observed. Ettringite hydrates begin to dehydrate within this temperature range. Moreover, it seems that the decomposition of ettringite lowers the OH^- concentration of the pore water solution. The $Ca(OH)_2$ crystals are sheet-like and have an elongated shape at ambient temperature. With a rise in temperature, the spatial distribution of $Ca(OH)_2$ crystals becomes more compact. It means smaller crystals occurring in a unit volume of the cement paste. This is connected by decreased solubility of $Ca(OH)_2$ at higher temperatures. By contrast, hydrated cement pastes at lower temperature are more likely to contain large masses of $Ca(OH)_2$, with a well-developed morphology. A rise in temperature affects the cement paste pore structure by reducing the specific surface of hydration products. Cement paste exposed to high-temperature attack is more heterogeneous in a microstructure and coarser in pore structure. The decrease in volume of the hydrate phase and $Ca(OH)_2$, and the coarsening of the pore structure of concrete are the main reasons influencing engineering properties decrease at high-temperature attack [62].

2.7.5 Aggregates characteristics and their significance for concrete

Aggregate is relatively inexpensive and does not enter into complex chemical reactions with water; it has been customary, therefore to treat it as an inert filler in concrete. However; due to increasing awareness of the role played by aggregates in determining many important properties of concrete, the traditional view of the aggregate as an inert filler is being seriously questioned [55].

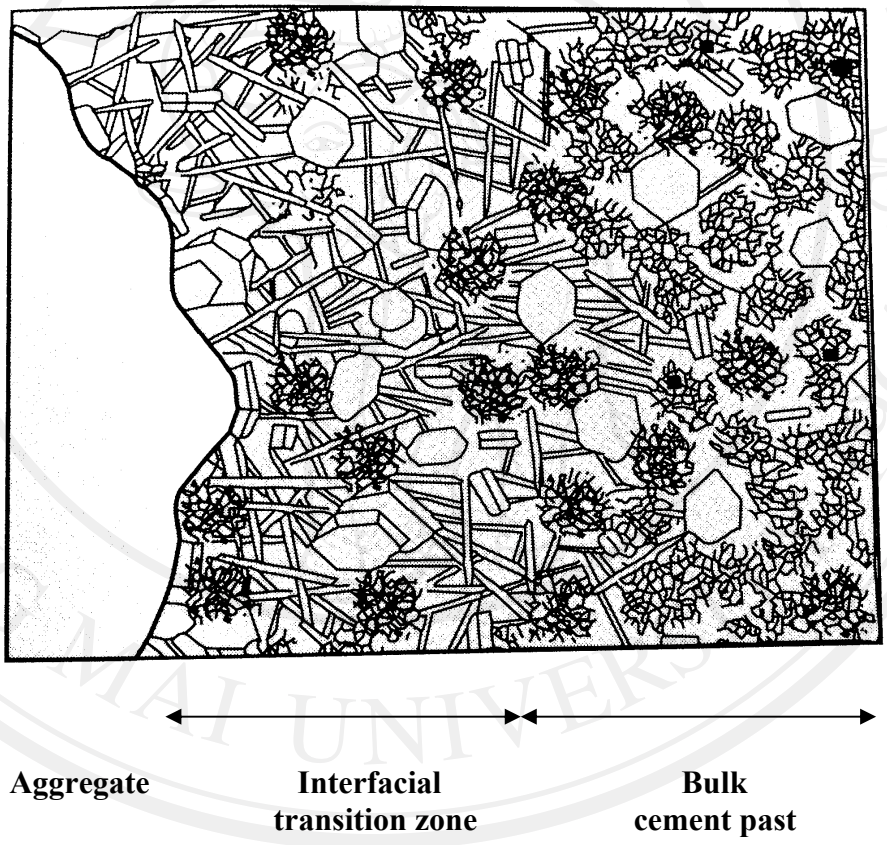

Fig. 2.9 The interface between the aggregate and cement paste [53].

The cement serves to bond the aggregate particles together and the nature of the interface between the aggregate and the cement is of great importance. The interfacial region between the aggregate and the cement is through to be very different from the bulk cement regions both in terms of morphology, density and composition. The structure is shown schematically in Fig. 2.9. This thickness of this interfacial region is about 50 μm, with the weakest part of the zone lying about 5 to 10 μm away from the interface [57]. The existence of this porous region can affect the fracture characteristics of the concrete and be a factor that limits the strength of the concrete. Some idea of the quality of the bond between the aggregate and cement can be obtained by inspecting a fractured sample of concrete. Ideally, there should be some fractured aggregate and some pull out. If all the aggregate has fractured, then the aggregate is too weak, and if all the aggregate has pulled out, then either the bond between the cement paste and the aggregate is too weak or the cement paste itself it too weak [58].

In order to be able to proportion suitable concrete mixes, each piece of aggregate (large or small) should be totally surrounded by cement, and the packing of the particles should be as dense as possible. The grading of the aggregate (the section of the particle size ranges to be used and the amount of aggregate in each range) should be such as to give the maximum density of particles packing which minimizes the amount of the more expensive cement used in the mix. These properties influence the paste requirements for workable fresh concrete [37].

Shape and surface texture of aggregate particles influence the properties of fresh concrete more than hardened concrete. Shape refers to geometrical characteristics such as round, angular, elongated, or flaky [55]. The relative quantities

of coarse and fine aggregate needed to give dense packing will depend on the shape of the aggregate particles. If the aggregate is angular, then the relative proportions of coarse/fine will be different than if it is rounded (spherical), because the random packing of coarse non-spherical particles results in a greater volume of void than the packing of coarse spherical particles and the void needs to be filled by fine particles [56]. On the other hand, angular aggregates will produce concrete of a greater strength than spherical aggregates. This is due to the greater surface area/volume ratio of angular aggregates which produces a larger bonding interface between the aggregate and the cement [59].

The surface texture, defined as the degree to which the aggregate surface is smooth or rough, is based on visual judgment. During early age, the strength of concrete, particularly the flexural strength, can be affected by the aggregate texture; a rougher texture seems to help the formation of a stronger physical bond between the cement paste and aggregate. At a later age, with a stronger chemical bond between the paste and the aggregate, this effect may not be so important [37].

Size and grinding of the aggregate is to minimize the void space between the aggregate, since this has to be filled with the cement. The selection of the relative amounts of the coarse and fine grades of aggregate is depending on many factors, which include the maximum size of the aggregate, the shape of the aggregate, the size distribution of the coarse and fine fractions, the workability required, the surface texture of the aggregate, the water/cement ratio to be used and the required strength of the concrete [55].

2.8 Composite materials

A "composite" is when two or more different materials are combined together to create a superior and unique material. Composite materials have found use in a number of structural applications, but their use in the electronics industry surprisingly widespread [63]. Such applications and advantages of composites electroceramics include there use in piezoelectric transducers, sensors, and actuators. Functional composites make use of a number of underlying the basic ideas, including the following: sum and product properties, connectivity patterns and percolation threshold. In most electronic devises there are several phases involved and a number of material parameters to be optimized. An electromechanical transducer, for example, may require a combination of properties such as large piezoelectric coefficient (d or g), low density and mechanical flexibility [23].

2.8.1 Properties and connectivity of composite materials

Properties of composite materials

For convenience, the properties such as physical and chemical properties of composites can be grouped as sum properties, combination properties, and product properties. The fundamental ideas underlying sum and product properties were introduced by van Suchtelen [64].

For sum properties, the composite property coefficient depends on the corresponding coefficients of its constituent phases. Thus the stiffness of a composite is governed by the elastic stiffnesses of its component phases and the mixing rule appropriate to its geometry. In general, the property coefficient of the composite will be between those of its constituent phases [65].

For combination properties, combining materials mean not only choosing component phases with the right properties for combining materials, but also coupling them in the best manner. Connectivity of the individual phases is of utmost importance, because this controls the properties of composites [65]. The basic mixing principle the properties of a composite between those of its constituent phases, but combination properties involve two or more coefficients which may average in a different way such as acoustic wave velocity determines the resonant frequency of piezoelectric devices. The velocity of waves propagating along the length of a long, thin rod and formula of velocity of waves is given by

$$\upsilon = (E/\rho)^{1/2} \qquad (2.10)$$

Where υ is acoustic wave velocity, E is Young's modulus and ρ is density [64].

Table 2.4 Examples of product properties [64].

Property of phase 1	Property of phase 2	Composite product property
Thermal expansion	Electrical conductivity	Thermistor
Magnetostriction	Piezoelectricity	Magnetoelectricity
Halle effect	Electrical conductivity	Magnetoresistance
Photoconductivity	Electrostriction	Photostriction
Superconductivity	Adiabatic demagnetization	Electrothermal effect
Piezoelectricity	Thermal expansion	Pyroelectricity

For product properties, the interaction of different properties in different component phases when combining materials resulted to product properties. The combination of two or more component (two or more constituents) of different properties sometimes yields surprisingly large third property as product properties. In fact, in a few cases, product properties are found in composites that were entirely absent in the phases that make up the composite [65]. The examples of product properties, including several described in this article are given in Table 2.4.

Connectivity of composite materials

The arrangement of the component phases within a composite is critical for the electromechanical properties of composites. Newnham et al. [65] have developed the concept of "connectivity" to describe the manner in which the individual phases are self-connected. In a diphasic system, there are ten types of connectivities in which each phase is continuous in zero, one, two or three-dimensions. The ten connectivities are denoted as the following 0-0, 0-1, 0-2, 0-3, 1-1, 1-2, 2-2, 1-3, 2-3 and 3-3.

It is conventional for the first digit to refer to the piezoelectrically active phase. Based on the connectivity designs, several important piezoelectric composites were developed. These connectivities are illustrated in Fig. 2.10 using a cube as the basic building block. For composites with 0-3 connectivity, the first number refers to that of the dispersed phase, and the second refers to that of the matrix phase. The "0" means that material is in the form of particles and the particles are not in contact with each other. The "3" means the matrix phase is self-connected in all three dimensions [66]. The major advantage of 0-3 is its ease of fabrication in a variety of forms including large flexible thin sheets, extruded bars and fibers, and molded shapes.

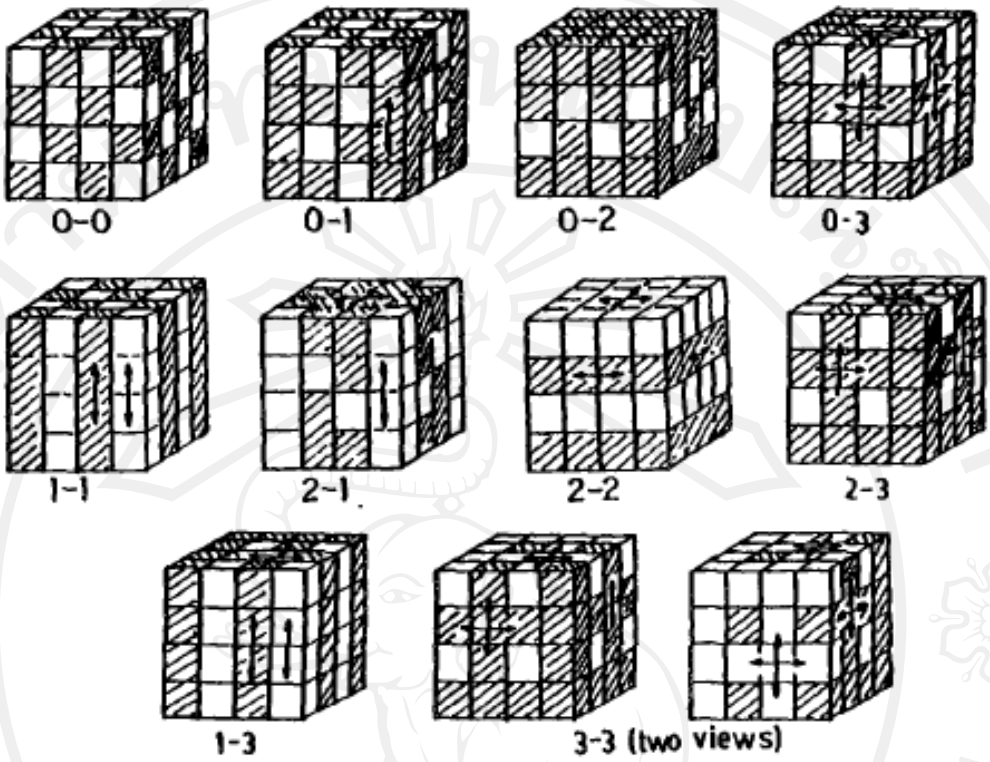

Fig. 2.10 Connectivity patterns in a diphasic composite system [66].

In composites with 1-3 connectivity, the ceramic phase is continuously connected in one dimension while the matrix phase is continuous in all three dimensions (self-connected in three dimensions). The ceramic component can be represented by a continuous row of particles, relatively long rods or fibres, or a parallel of discs. The 1-3 piezoelectric composites present interesting examples of volume fraction dependencies of the effective piezoelectric properties. The 1-3 piezoelectric composites that exhibit high performance find various applications, mainly as active elements of active elements of hydrophones, actuators, sensor, ultrasonic transducers, medical-imaging devices [67].

For composites with 2-2 connectivity, the ceramic phase and matrix phase are continuously connected in two dimensions. Another type of connectivity well suited

to processing is the 2-2 pattern made up of alternating layers of the two phases. In this arrangement both phases are self-connected in the lateral X and Y directions but not connected perpendicular to the layers along Z [68]. The 2-2 piezoelectric composites find various applications, for example, as active elements of sensors, actuators and transducers for medical-imaging applications [67].

2.8.2 Models of composites

A number of models have been proposed and used for predicting the effects of second phases on the properties of the composite.

Series model

To illustrate the major modifications in ensemble properties which can be effected even in simple linear systems, one-dimensional solutions are presented for the dielectric and piezoelectric properties of heterogeneous two-phase structures [23].

$$\varepsilon = \frac{{}^{1}\varepsilon \cdot {}^{2}\varepsilon}{{}^{1}v\,{}^{2}\varepsilon + {}^{2}v\,{}^{1}\varepsilon} \qquad [69] \qquad (2.11)$$

Where ε, ${}^{1}\varepsilon$ and ${}^{2}\varepsilon$ are the dielectric constant of the composite, the phase 1 and the phase 2, respectively. The ${}^{1}v$ and ${}^{2}v$ are the volume fraction of the phase 1 and the phase 2, respectively [69].

Consider first the piezoelectric properties of lamellar diphasic composites. Longitudinal piezoelectric coefficient d_{33} has been derived for a diphasic piezoelectric with the constituent phases arranged in alternating layers normal to the x_3 direction (Fig. 2.11(a)). Designating phase 1 with a subscript 1, and phase 2 with a subscript 2, phase 1 has volume fraction ^{1}v**,** piezoelectric coefficient ${}^{1}d_{33}$ and dielectric constant

${}^{1}\varepsilon$, and phase 2 has ${}^{2}v$, ${}^{2}d_{33}$ and ${}^{2}\varepsilon$, respectively. Solving for the piezoelectric coefficient of the composites gives [23].

$$d_{33} = \frac{{}^{1}v.{}^{1}d_{33}.{}^{2}\varepsilon + {}^{2}v.{}^{2}d_{33}.{}^{1}\varepsilon}{{}^{1}v.{}^{2}\varepsilon + {}^{2}v.{}^{1}\varepsilon} \qquad [65] \qquad (2.12)$$

${}^{1}g_{33}$ and ${}^{2}g_{33}$ are piezoelectric voltage coefficient of phase 1 and phase 2, respectively [65].

$$g_{33} = \frac{{}^{1}v^{1}d_{33}}{{}^{1}\varepsilon} + \frac{{}^{2}v^{2}d_{33}}{{}^{2}\varepsilon} \qquad [65] \qquad (2.13)$$

It is interesting to note that for series connection even a very thin low-permittivity layer rapidly lowers the d-coefficient but has little effect on the corresponding g-coefficient [23].

Parallel model

The parallel models present the extreme cases where the model is alternating layers of each phase, parallel to the applied field (Fig. 2.11(b)), again for the one-dimensional case and neglecting transverse coupling, the composite dielectric constant and piezoelectric coefficient are given by

$$\varepsilon = {}^{1}v^{1}\varepsilon + {}^{2}v^{2}\varepsilon \qquad [69] \qquad (2.14)$$

$$d_{33} = \frac{{}^{1}v^{1}d_{33}\,{}^{2}S_{33} + {}^{2}v^{2}d_{33}\,{}^{1}S_{33}}{{}^{1}v^{2}S_{33} + {}^{2}v^{1}S_{33}} \qquad [65] \qquad (2.15)$$

Where ${}^{1}S_{33}$ and ${}^{2}S_{33}$ are the elastic compliances for stresses normal to the electrode of phase 1 and phase 2, respectively [65]. For the voltage coefficient is given by

$$g_{33} = \frac{{}^{1}v^{1}d_{33}\,{}^{2}S_{33} + {}^{2}v^{2}d_{33}\,{}^{1}S_{33}}{\left({}^{1}v^{2}S_{33} + {}^{2}v^{1}S_{33}\right)\left({}^{1}v^{1}\varepsilon + {}^{2}v^{2}\varepsilon\right)} \qquad [65] \qquad (2.16)$$

A composite of interest here is that of an elastically compliant non piezoelectric in parallel with a stiff piezoelectric.

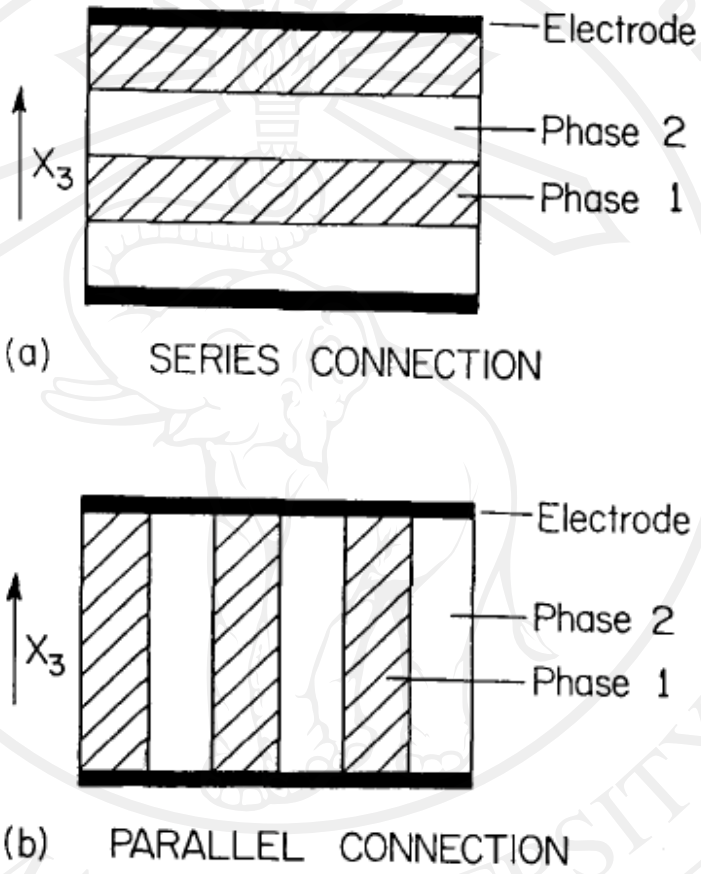

Fig. 2.11 The model used in estimating the piezoelectric effect of diphasic solid; (a) series model and (b) parallel model [65].

Cube model

A concept of connectivity was introduced by Newnham *et al.* in 1978 [65] and the composites have been classified according to this concept. They have also derived theoretical equations for the piezoelectric coefficient of the composites from series and parallel models. Banno *et al.* [70] has introduced a modified cubes model, which

generalizes the parallel, series and cube models. The modified cubes model was used to calculate the thickness and dielectric constant of the surface layer. The unit cell of the composite consists of a ceramic particle (phase 1) and the matrix (phase 2) as shown in Fig. 2.12.

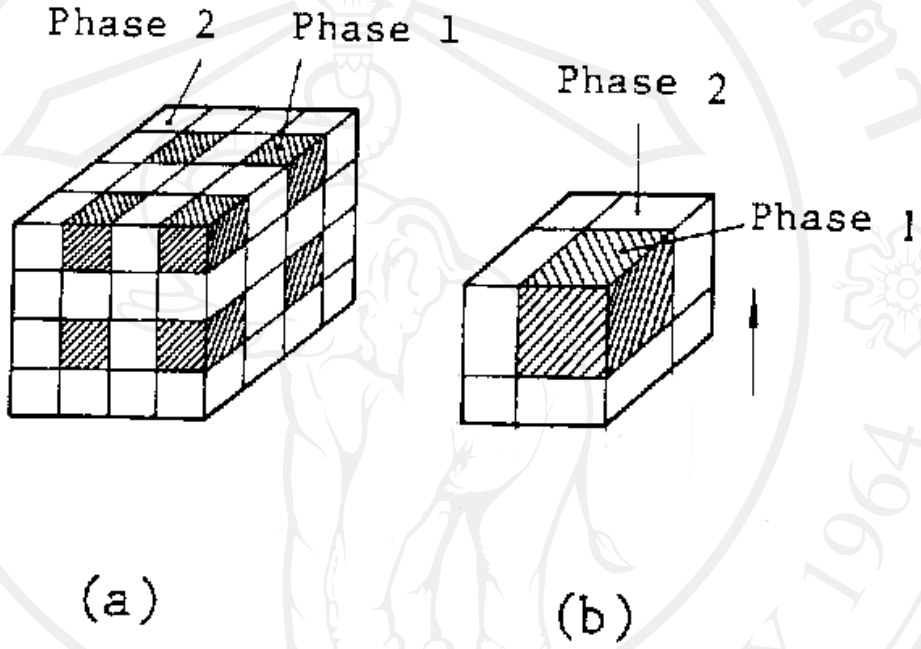

Fig. 2.12 (a) A composite with 0-3 connectivity and (b) Unit modified cubes cell of composite with piezoelectric ceramic particle (oblique lined area) without surface layer [71].

The modified cubes model becomes equivalent to the parallel, series, and cube model in the cases when Y = 1, X = 1 and X = Y = 1 respectively. As shown in Fig. 2.13(a) obtain a unit cube cell equivalent to the unit cell illustrated in Fig. 2.12 and Fig. 2.13(b) shows schematic representation for the modified cube model which is divided into two parts [70-71].

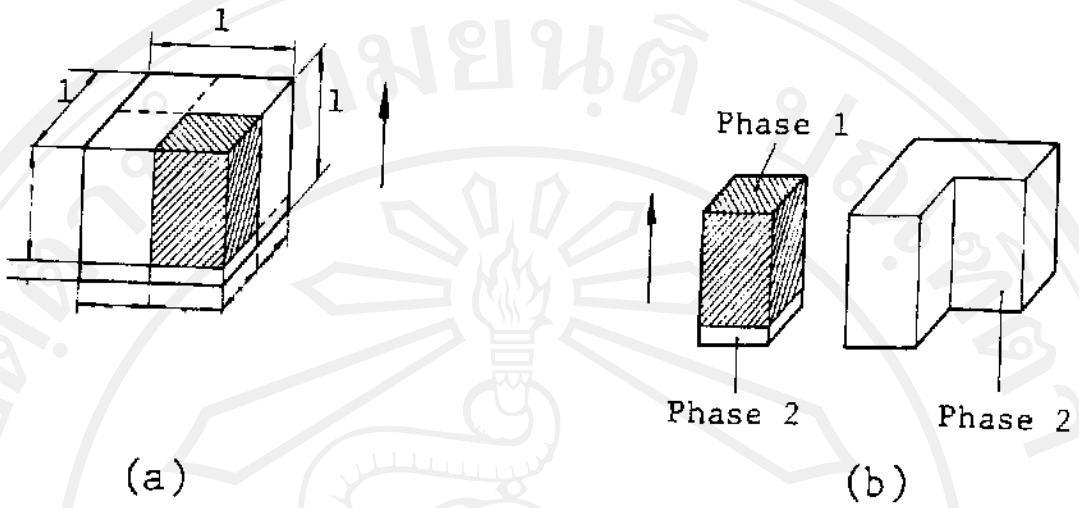

Fig. 2.13 (a) A unit cubes cell equivalent to the unit cell equivalent to the unit cell illustrated in Fig. 2.12 (b) and (b) schematic representation for the modified cube model which is divided into two parts [70].

For the cube model, Banno [70] proposed a "modified cube model," which took into account the anisotropic distribution of cubes in x, y, and z directions, which based on fundamental principal of the physical mixing. The mathematical equations of cube (Eq. (2.17)) model for dielectric constant are described as follows [72]:

$$\varepsilon_C = \frac{{}^1\varepsilon \cdot {}^2\varepsilon}{\left({}^2\varepsilon - {}^1\varepsilon\right){}^1v^{-1/3} + {}^1\varepsilon \cdot {}^1v^{-2/3}} + {}^2\varepsilon \cdot \left(1 - {}^1v^{2/3}\right) \quad [69] \qquad (2.17)$$

The theoretical equations of cube (Eq. (2.18)) model for the d_{33} values can be denoted as follows [70]:

$$d_{33} = \frac{{}^1d_{33}\,{}^1v}{\left({}^1v^{1/3} + \frac{{}^1\varepsilon}{{}^2\varepsilon}(1 - {}^1v^{1/3})\right)(1 - {}^1v^{1/3} + {}^1v)} \quad [77] \qquad (2.18)$$

For the piezoelectric voltage coefficient from (Eq. (2.17)) and (Eq. (2.18)) is given by

$$g_{33} = \frac{{}^{1}d_{33}\,{}^{1}v}{\left({}^{1}v^{1/3} + \frac{{}^{1}\varepsilon}{{}^{2}\varepsilon}(1-{}^{1}v^{1/3})\right)(1-{}^{1}v^{1/3}+{}^{1}v)} \times \frac{({}^{2}\varepsilon-{}^{1}\varepsilon)\,{}^{1}v^{-1/3}+{}^{1}\varepsilon\,{}^{1}v^{-2/3}}{{}^{1}\varepsilon\,{}^{2}\varepsilon+\left[{}^{2}\varepsilon\left(1-{}^{1}v^{2/3}\right)\right]\left[\left({}^{2}\varepsilon-{}^{1}\varepsilon\right){}^{1}v^{-1/3}+{}^{1}\varepsilon\,{}^{1}v^{-2/3}\right]} \quad (2.19)$$

The schematic configurations of series, parallel and cubic models are represented in Fig. 2.14.

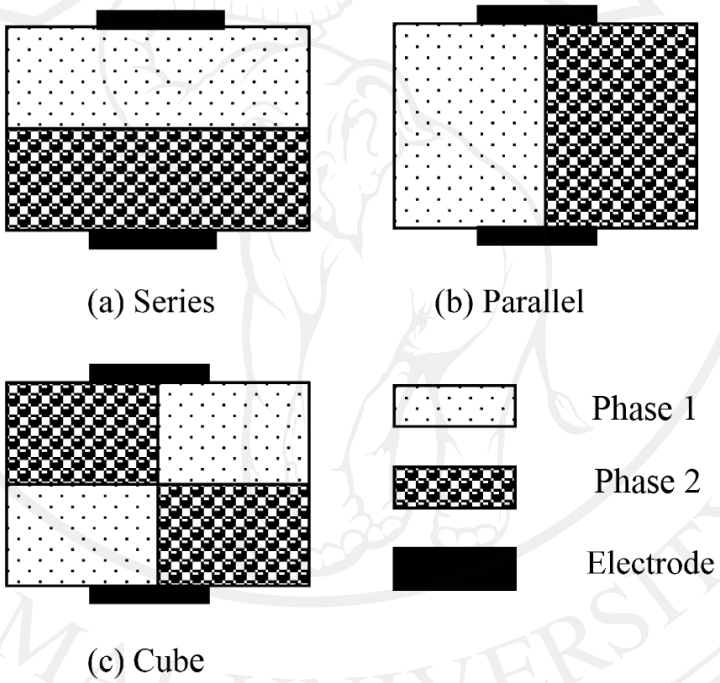

Fig. 2.14 Illustration of the series, parallel, and cube models for composite [69].

2.9 Literature review of piezoelectric-cement based composites

For some important modern structures, such as high rise buildings, large span bridges, dams, and so on, severe vibration and significant internal damage may be caused by dynamic loading from different sources, such as a strong wind or earthquake. This will pose a great threat to the safety of the structures. Therefore, in recent years, structural health monitoring has attracted much attention in civil

engineering. Real-time structural health monitoring can provide instantaneous information on the condition of a specified structure, which will result in a significant increase of the safety margin and reductions in maintenance cost. The essential components for such health monitoring are sensors and actuators which are made of the so-called smart materials. However, the traditional smart materials, such as piezoelectric ceramic, shape memory alloys, and piezoelectric polymer, may not be applicable in civil engineering due to the distinct differences in the properties between the smart materials and the concrete structures [1-2].

Furthermore, the piezoelectric ceramic such as lead zirconate titanate (PZT) exhibit high acoustic impedance ($\approx 30 \times 10^6$ kg/m^{2}s) [7] compared to that of concrete ($\approx$6.9-11 x 10^6 kg/m^{2}s) [13-14]. Some factors during the hydration of cement such as variations in relative humidity or temperature and chemical reactions, will cause shrinkage or expansion of concrete. Such mismatching would not only degrade the energy transfer between the traditional smart materials and the host concrete, but also cause considerable lost of the signal transmission [1]. Therefore, some kinds of smart materials should be developed to meet the requirement of the civil engineering main structure material, concrete. As the techniques used in sensors and actuators, piezoelectricity has been proved to be one of the most efficient technologies for most applications in smart structures. And it has attracted great attention in research activities towards the applications of sensors and actuators in civil engineering [1-11].

0-3 Piezoelectric-cement based composites

Therefore, the kinds of smart materials suitable for applications in civil engineering structures should have good piezoelectric properties as well as good

compatibility. The first reported cement-based 0-3 piezoelectric composites using piezoelectric lead zirconate titanate (PZT) to fabricate piezoelectric-cement composites was by Li *et al*. [3]. In 2002, they studied two sizes of PZT ceramic particles mixed with Portland white cement to make the 0-3 piezoelectric composite to investigate the effects of the particle size of PZT on the piezoelectric properties of the PZT/cement composites. Various percent by volume of PZT were mixed and spreaded into Portland cement. The result showed that the dielectric constant of the composites falls between the predictions of the cubes model and the series model, which means that the PZT particles in the composites were uniformly dispersed (see in Fig. 2.15).

The 0-3 piezoelectric-cement based composites were shown to have a slightly higher piezoelectric factor and electromechanical coefficient than those of 0-3 PZT-polymer composites and adequated for sensor application. Moreover, it was found that the coarser PZT particles lead to a higher d_{33} in the composites. When the particle size of embedded PZT powder was decreased, the piezoelectric coefficient (d_{33}), dielectric constant (ε_r) and electromechanical coupling coefficient (K_t) of the PZT/cement composite were all decreased. Moreover, it can be tuned to acoustic impedance to match the host structure material, i.e., concrete. Their research indicates that, when the 40-50 %PZT composites, the acoustic impedance of the 0-3 composite can match that of concrete in Fig. 2.16. Furthermore, the advantage of the acoustic matching not only the available sensors placed outside a structure is that these sensors but also can be placed inside the concrete structure for real-time structure monitoring in order to detect vibration of the host structure material, concrete [3].

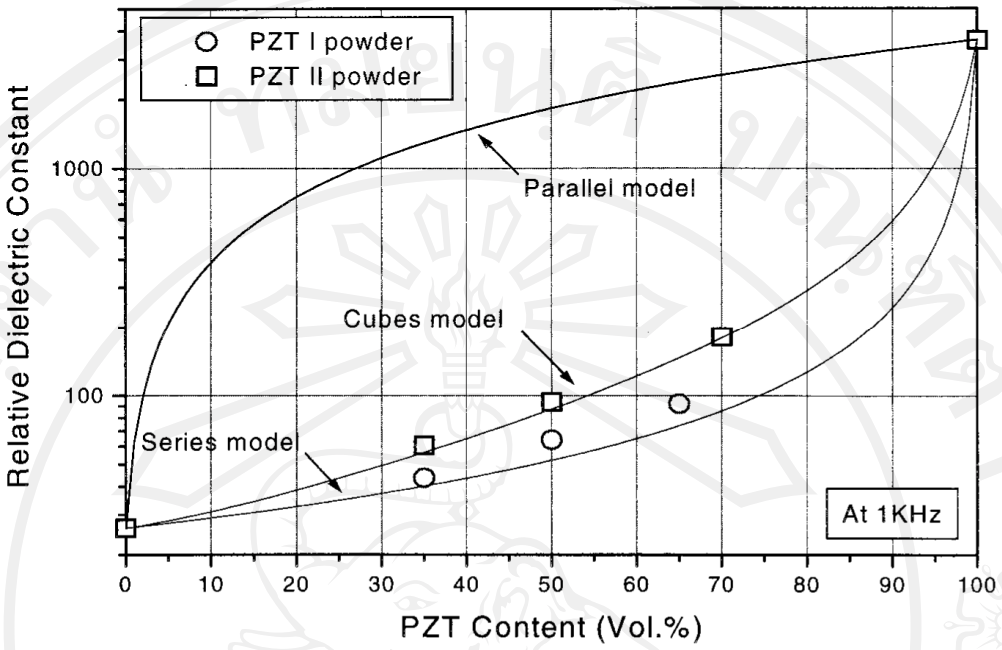

Fig. 2.15 Relative dielectric constant versus PZT particles content [3].

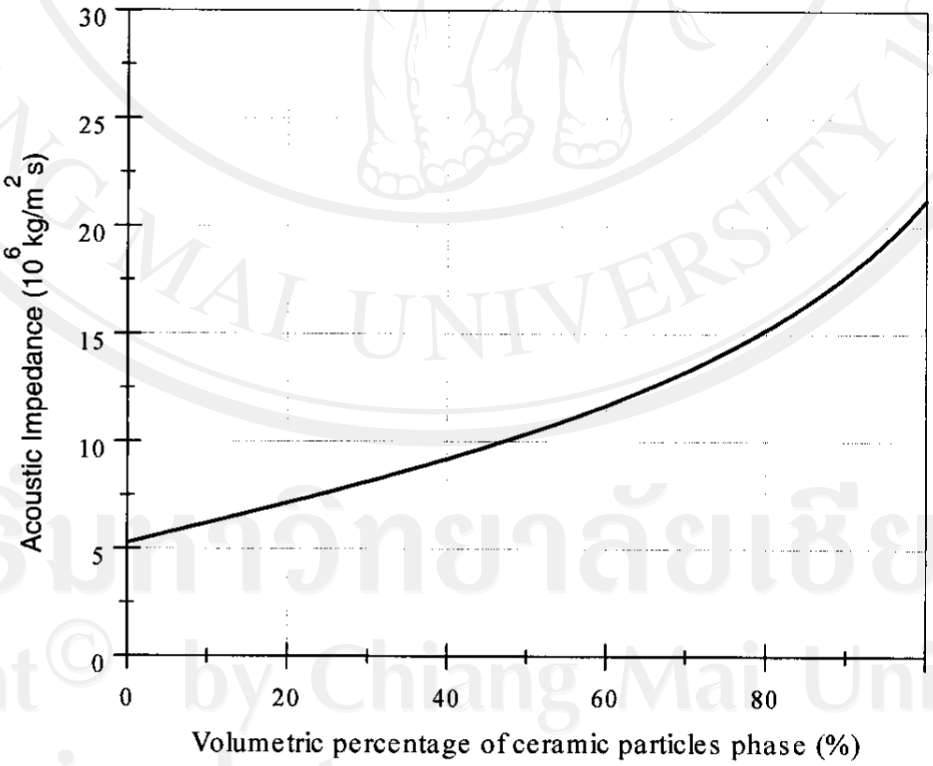

Fig. 2.16 Acoustic impedance versus PZT particles content [3].

In 2005, Xin *et al*. [4] have studied 0-3 piezoelectric using a sulphoaluminate cement and lead magnesium niobate (PMN) ceramic particles. Piezoelectric and dielectric properties of the composites with different PMN contents were investigated. The specimens were put in a curing room with a temperature of 20ºC for 3 days before measurements. Then, the poling was carried out under optimum poling field of 4kV/mm at 130ºC in a stirred silicone oil bath. From their results, the d_{33} values of the 0-3 piezoelectric-cement composites showed a roughly nonlinear increase as a function of the PMN content. The electromechanical coupling factor (K_p and K_t) of composites increased with increasing the content of PMN.

Moreover, in 2006 Huang *et al.* [2] studied the preparation and polarization of 0-3 cement based piezoelectric composites. The specimens were put in a curing room with a temperature of 20ºC and relative humidity of 100% for 3 days before measurements. The result showed that the optimum poling field, poling time and poling temperature were 4.0 kV/mm 45 min and 120 °C, respectively. The result exhibited that, in the course of the poling, the leakage current was chiefly caused by the interface pore, the cement matrix pore and their inner water which has a significant influence on the degree of the poling.

In 2007, Chaipanich [5] studied the effect of PZT particle size on dielectric and piezoelectric properties of 0-3 PZT-cement composites. PZT of various median particle size (3.8-620 μm) were used at 50% by volume to produce the composites. Table 2.5, it was showed that ε_r and d_{33} values both increased with increasing the PZT particle size. The enhancement in the dielectric and piezoelectric properties was contributed to lesser contacting surface between the cement matrix and the PZT particle. A Summary of the results reported in comparison to the previous works

under similar poling conditions at the same PZT volume content of 50% is given in Table 2.5. The size of PZT particle size used is also stated. From our result it was cleared that the particle size of PZT has an effect on the properties of the PZT-cement composites.

Table 2.5 Summary of the results in comparison to the previous works [5]

Reference	**PZT particle size (μm)**	ε_r	$tan\ \delta$	d_{33} **(pC/N)**
Li et al. [3]	4.9	64	-	9.5
	83.5	94	-	12.5
Li et al. [72]	83.5	300	-	23
Huang et al. [73]	166.5	-	-	7
Chaipanich [5]	3.8	167	0.95	17
	148.8	170	0.83	22
	620	176	0.79	26

Chaipanich [74] studied the fabrication and properties of PZT-ordinary Portland cement composites in 2007. The PZT ceramic particles were then mixed with Portland cement (OPC) using PZT at 40%, 50% and 60% by volume and pressed together at 80 MPa to produce 0-3 connectivity PZT-OPC composite discs of 15 mm in diameter and 2 mm in thickness. Thereafter, the composites were placed for curing at 60 °C and 100% relative humidity for 3 days in order to obtain a steady and rigid form similar to hardened cement paste. These results reported the piezoelectric coefficient were highest so far for PZT-cement composite poled at not more than 2 kV/mm. Moreover, using this fabrication method it was possible to produce PZT-

OPC composites with more than 50% PZT by volume and that these composites have good potential for use in structural applications.

In 2008, the effects of poling temperature on the piezoelectric properties such as piezoelectric coefficient (d_{33}) and electromechanical coupling coefficient (K_t) of 0-3 connectivity PZT-Portland cement (PC) composites were investigated by Jaitanong *et al.* [75] PZT-PC composites were produced using PZT of 50% by volume and the poling temperatures were selected at 100 °C, 130 °C and 160 °C. The results showed that when using the poling temperature at 130 °C, the d_{33} and K_t values were found to be highest at 13 pC/N and 19.39%, respectively (see in Fig. 2.17, 2.18 and 2.19, Respectively).

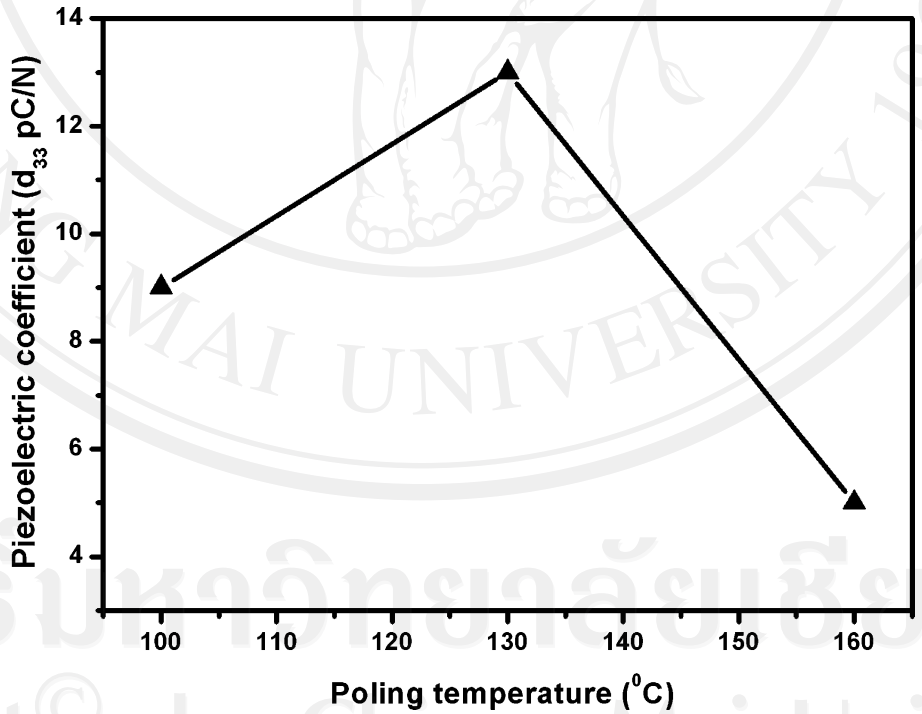

Fig. 2.17 The effect of poling temperature on the piezoelectric coefficient (d_{33}) [75].

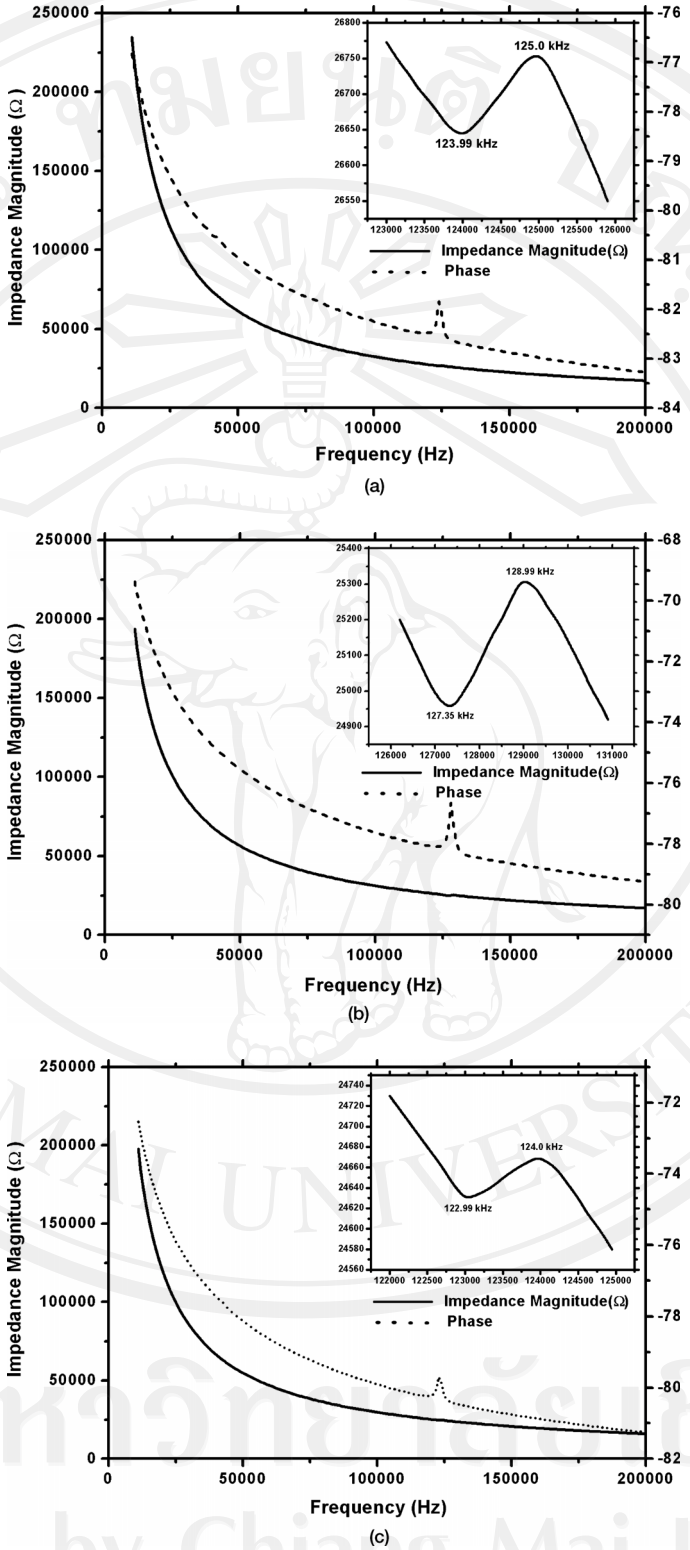

Fig. 2.18 The impedance magnitude and the phase spectra of PZT-PC composites; (a) poling temperature at 100 ºC, (b) poling temperature at 130 ºC and (c) poling temperature at 160 ºC [75].

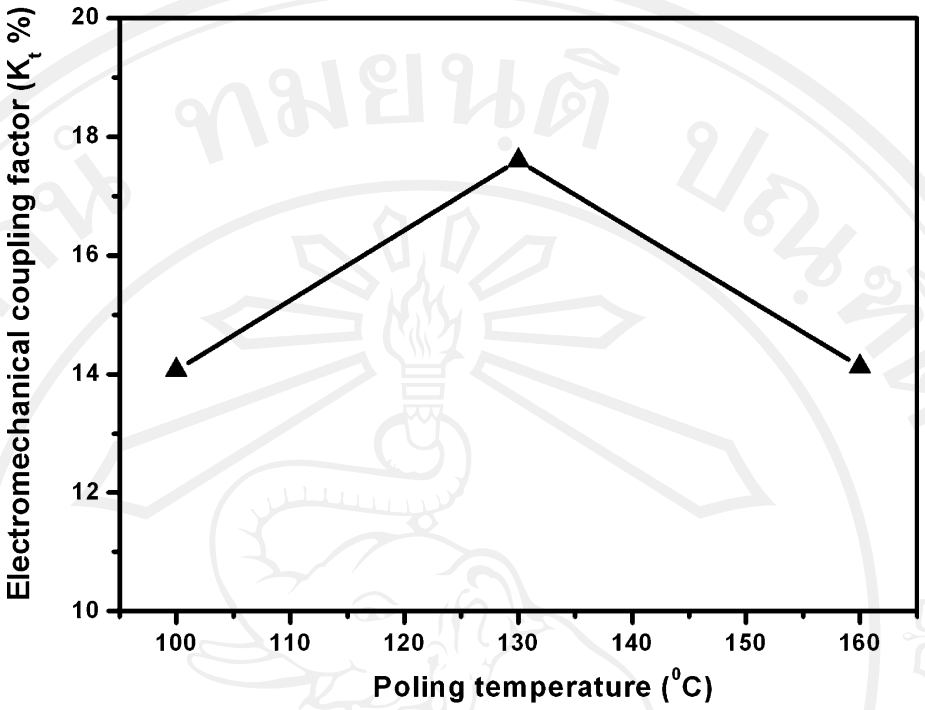

Fig. 2.19 Relationship between the K_t and the poling temperature [75].

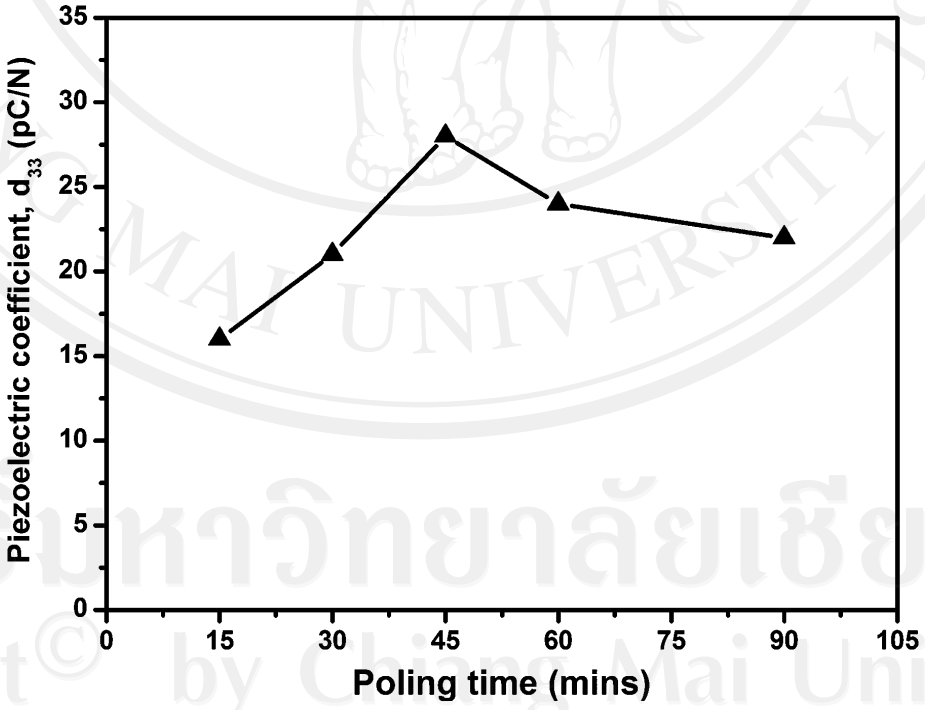

Fig. 2.20 The effect of poling time on the piezolecletric coefficient (d_{33}) [76].

Furthermore, Chaipanich *et al*. [76] investigated the effect of poling time on the piezoelectric properties such as d_{33}, impedance magnitude and phase spectra, and K_t values of 0-3 connectivity PZT-Portland cement (PC) composite. In 2008, the PZT-PC composites were produced using PZT of 60% by volume and the poling time of 15, 30, 45, 60 and 90 minutes were used. The results showed that when using the poling time at 45 minutes, the d_{33} (Fig. 2.20) and K_t values were found to be highest at 28 pC/N and 19.87%, respectively. In the same year (2008), Xing *et al*. [77] also studied dielectric, piezoelectric, and elastic properties of cement-based piezoelectric ceramic composites. The influence of the component of composite on the material properties were studied in detail. The piezoelectric constant and compressive (Fig. 2.21) of composites was found to increase with increasing PZT content.

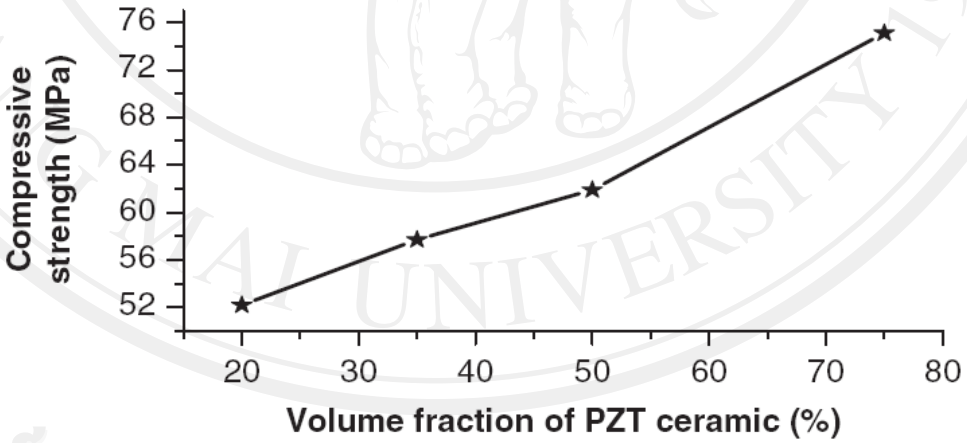

Fig. 2.21 The compressive strength versus volume fraction of PZT ceramic in composites [77].

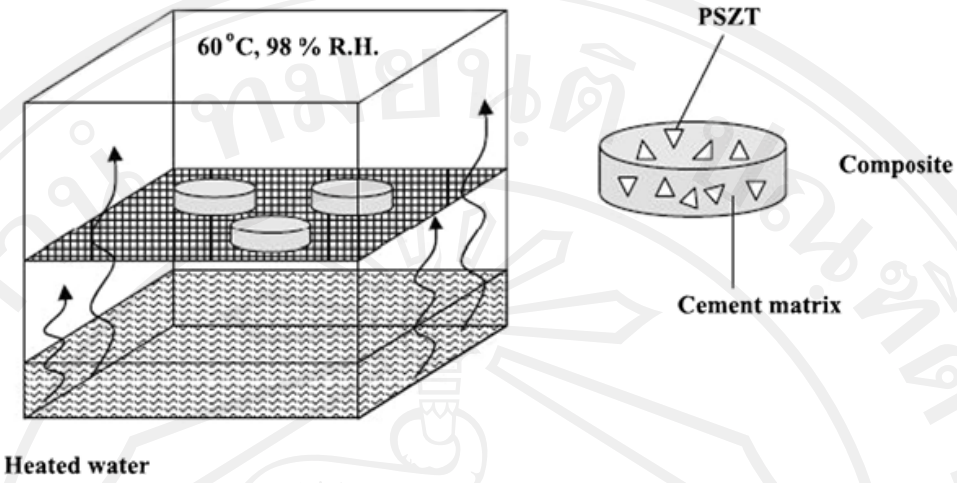

Fig. 2.22 Curing chamber with controlled environment of 60°C and 98% RH [81].

In additional, Chaipanich *et al*. [78] studied properties of Sr- and Sb-doped PZT-Portland cement composites in 2009. PZT was doped with Sr and Sb (PSZT) was mixed with normal Portland cement to produce 0-3 connectivity PSZT-Portland cement composite using PSZT contents of 50% and 70% by volume. The composites were pressed into discs of 10 mm in diameter and 2 mm in thickness and cured for 3 days in a controlled 60°C, 98% relative humidity (RH) environment (Fig. 2.22) before measurements. SEM micrographs of PSZT50 and PSZT70 composites are shown in Fig. 2.23. Scanning electron micrographs show PSZT ceramic particles closely surrounded by the hydrated cement matrix where a dense microstructure can be observed in the interfacial zone. Both the ε_r and d_{33} values were found to increase with PSZT content and the values are amongst the highest so far for these types of composites, where the ε_r and d_{33} values reached 590 and 48 pC/N, respectively.

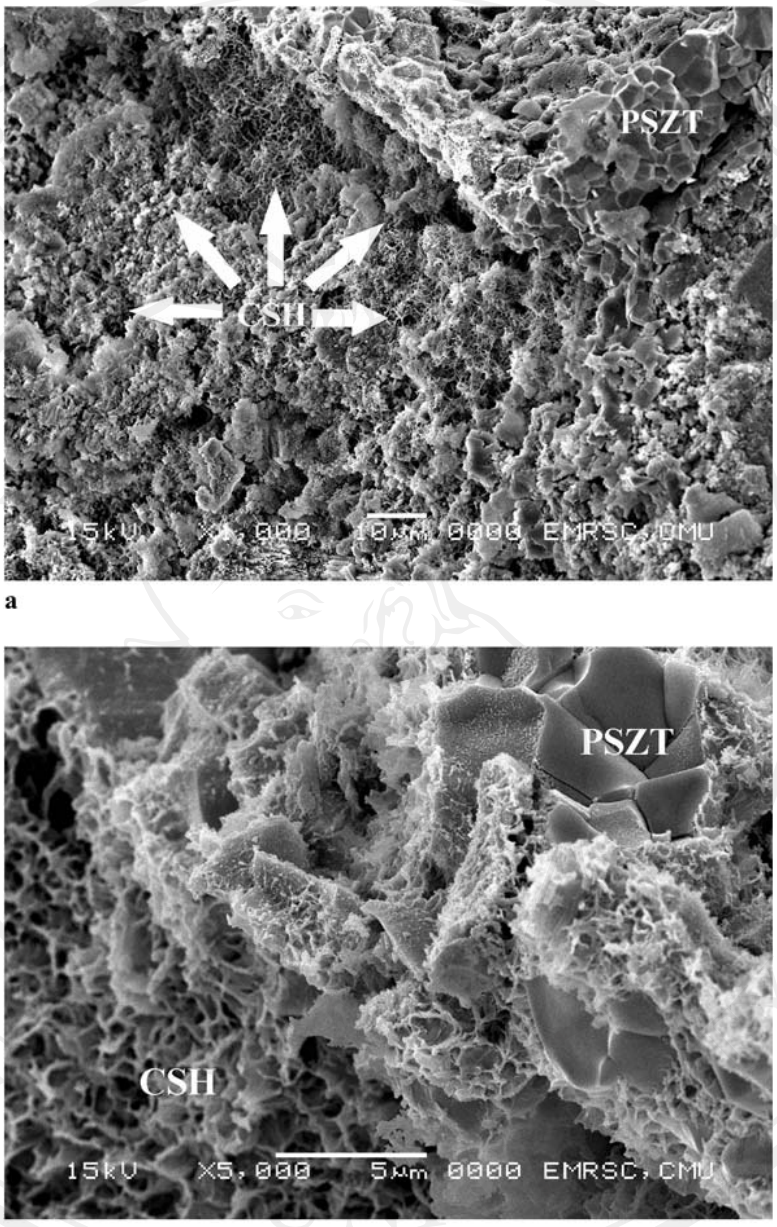

Fig. 2.23 SEM micrographs of PSZT70-PC composite; (a) ×1000 magnification and (b) ×5000 magnification [78].

In 2011, Jaitanong [79] studied electrical properties of piezoelectric ceramic-Portland cement composites. The lead zirconate titanate ceramic (PZT) was used as a ceramic-phase mixed with Portland cement to 0-3 connectivity cement-based

piezoelectric composites. For part of 0-3 PZT-PC composites, the results showed that the electrical properties of the composites increased with piezoelectric ceramic particle size. The results are given in Table 2.6.

Table 2.6 Electrical properties of cement piezoelectric composites [79].

Materials	Vol%	ε_r (at1 kHz)	d_{33} (pC/N)	g_{33} (10^{-3}Vm/N)	ρ (10^3kg/m^3)	Ref
PZT-SH	100	3643	513	15.9	7.5	[3]
Cement paste	100	~56	-	-	~2.0	[3]
Concrete	100	-	-	-	~2.4	[3]
PZT-PC	50:50	94.2	12.5	15.0	3.73	[80]
PZT	100	~1000	198	21	8.0	[79]
PZT- PC	50:50	374	18	16	5.57	[79]

The enhancement in the electrical properties was contributed to less contacting surface between the cement matrix and the piezoelectric ceramic particles. Furthermore, piezoelectric ceramic of median size of 450 μm can be produced and it gave the highest electrical properties. The property of ceramic and the volume ratio of ceramic/cement will affect d_{33} and g_{33} value greatly and higher content of piezoelectric ceramics is results in higher d_{33} and g_{33} value in 0-3 type cement-based PZT composites.

In 2013, Chaipanich *et al.* [81] studied the compressive strength and microstructure of 0-3 lead zirconate titanate ceramic-Portland cement composites. PZT-PC composites containing 40%, 50% and 60% of PZT by volume were produced

and their mechanical and hydration properties were investigated. Compressive strength results typical of those used in normal concrete were found at 41.5-45.0 MPa for all PZT-PC composites, and therefore would be able to resist the same mechanical loading as would the concrete host structure. The compressive strength results were found to increase when PZT volume increases from 40% to 60% (Fig. 2.24). Using thermal analysis, calcium silicate hydrates, ettringite and calcium hydroxide, all of which are cement hydration products, were detected.

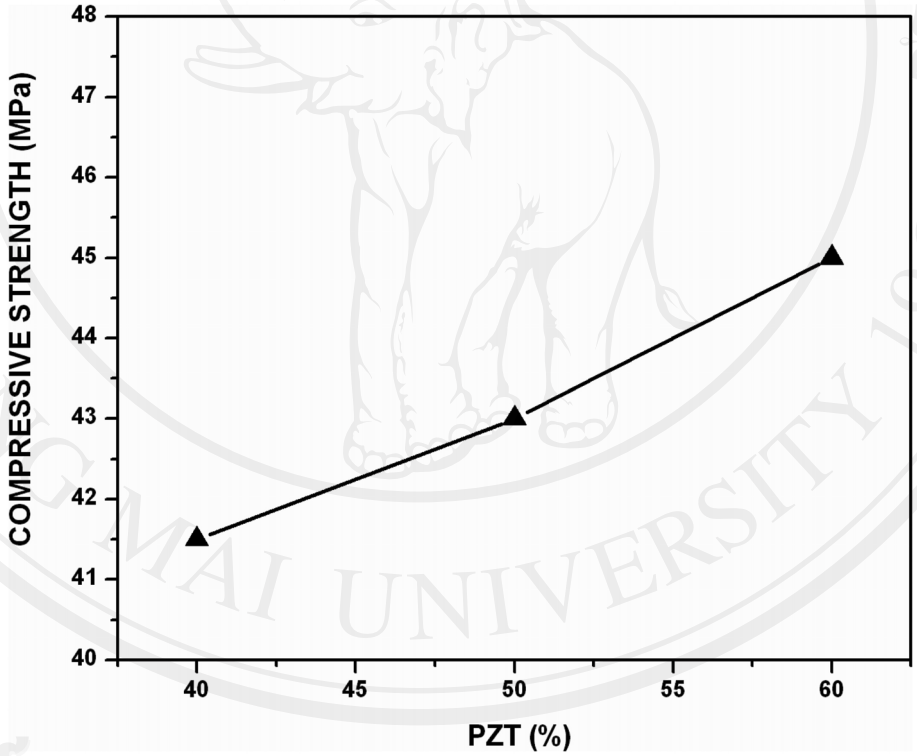

Fig. 2.24 Compressive strength results of PZT-PC composites [81].

1-3 Piezoelectric-cement based composites

The past research of the piezoelectric composite mainly concentrates on these connection types, such as 0-3, 1-3, and 2-2. In 2005, Lam *et al.* [7] studied

piezoelectric cement-based 1-3 composites. The composites with different volume fractions of PZT ranging from 0.25 to 0.77 were fabricated by the dice-and-fill method. It was found that the 1-3 composites have good piezoelectric properties that agreed quite well with theoretical modeling. The thickness electromechanical coupling coefficient could reach 0.55 in the composite with a ceramic volume fraction of 0.25. Those composites have potential to be used as sensors in civil structure health monitoring systems.

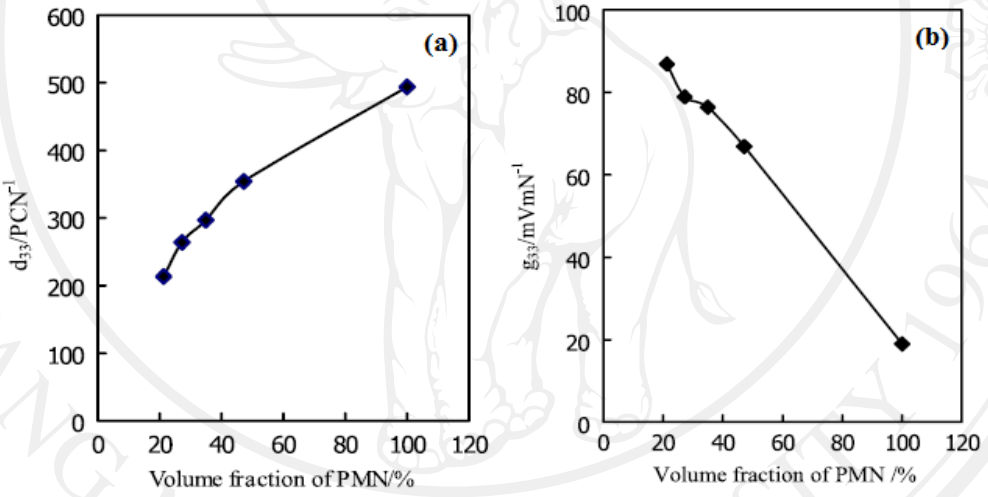

Fig. 2.25 The relationship between the piezoelectric constant and volume fraction of PMN; (a) d_{33} values and (b) g_{33} values [82].

Li *et al*. [82] studied an investigation on 1-3 cement based piezoelectric composites in 2007. The 1-3 PMN (lead magnesium niobate)- sulfoaluminate cement composites which had good compatibility with civil engineering structural materials were fabricated by the cut-fill technique. The results showed that the d_{33} and ε_r values of the composites increase linearly with the increase of PMN volume fraction. The g_{33} values of the composites were much higher than those of pure PMN (see in Fig. 2.25).

The remnant polarization P_r and the coercive field E_c of the composite with 27.26% volume fraction of PMN are 4.12 μCcm^{-2} and 4.01 kVmm^{-1}, respectively. By enhancing the PMN volume fraction, the acoustic impedance of the composites can be tailored to match that of the civil engineering structural material, i.e. concrete.

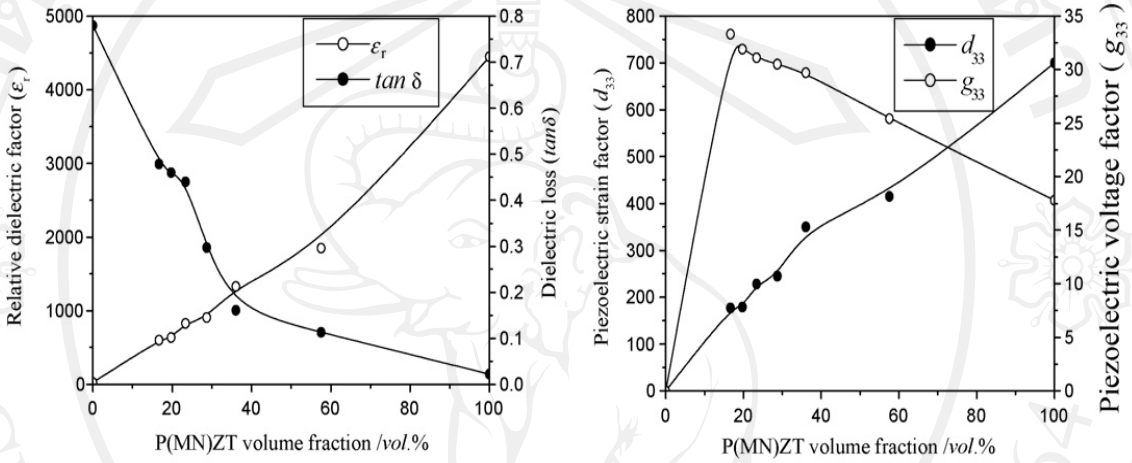

Fig. 2.26 Variation of (a) dielectric properties and (b) piezoelectric properties of 1-3 piezoelectric ceramic–cement composites as a function of P(MN)ZT ceramic volume fraction [8].

Furthermore, Xin *et al*. in 2010 [8] studied the performance investigation of the 1-3 piezoelectric ceramic-cement composites. The 1-3 piezoelectric ceramic-cement composites has been fabricated using sulphoaluminate cement and lead niobium-magnesium zirconate titanate ceramics (P(MN)ZT) as matrix and functional component, respectively. The composites were fabricated by cutting-filling technique and cured in moisture for 7 days. From their results, it was found that both ceramic volume fraction and shape parameters of the piezoelectric ceramic component were shown to be adjustable to make the composite compatible with concrete. Moreover,

ceramic volume fraction has a great influence on piezoelectric, dielectric and acoustic impedance properties of the composites. The results are showed in Fig. 2.26 and Table 2.7, respectively.

Table 2.7 Electromechanical and acoustic impedance properties of 1-3 piezoelectric ceramic-cement composite with P(MN)ZT ceramic volume fraction [8].

P(MN)ZT ceramic volume fraction (vol.%)	t (mm)	ρ ($\times 10^3$ kgm^{-3})	v_c (ms^{-1})	Z (M rayl)	K_p (%)	K_t (%)	Q_m
100	5	7.45	4560.00	30.00	65.00	46.00	70.00
57.57	5	3.37	3525.38	11.88	43.14	55.84	13.35
36.05	5	2.89	3300.38	9.54	44.94	57.20	12.24
28.72	5	2.53	3450.38	8.73	43.14	50.43	8.47
23.39	5	2.31	3300.38	7.62	43.14	54.45	8.39
19.75	5	2.12	3375.38	7.16	41.72	43.10	8.50
16.67	5	2.00	3300.38	6.75	41.72	43.30	7.16

Chaipanich *et al.* [9] also studied the dielectric and ferroelectric hysteresis properties of 1-3 lead magnesium niobate-lead titanate ceramic/Portland cement composites (1-3 PMN-PT/PC composites) in 2012. The composites were placed for curing at 60 °C and 98% relative humidity before measurements. The result showed that the dielectric constant at 1 kHz of the PMN-PT/PC composite was found to be 1500. The ‘‘instantaneous’’ remnant polarization (P_{ir}) at 50 Hz and at the electric field of 7 kV/cm of the PMN-PT/PC composite was found to be 10 μC/cm^2. At a similar frequency and electric field used, these values of 1-3 composite were found to

be significantly higher than previously published results of 0-3 composites. It was believed that 1-3 composites essentially contain the piezoelectric ceramic fully aligned in one direction which allows the ceramic to possess greater dielectric properties and ferroelectric behavior giving less loss that would otherwise occurred in the 0-3 composites. In 0-3 composites, the piezoelectric ceramic existed as random particles surrounded by cement matrix with high loss caused by the conducting ions. In addition, less contact surface areas between the two materials would improve the properties of 1-3 composites when compared to 0-3 composites having the same volume content of ceramic.

2-2 Piezoelectric-cement based composites

In 2007, Huang *et al.* [10] studied fabrication and properties of 2-2 cement based piezoelectric composites. The composites with 2-2 connectivity were fabricated from PMN ceramic and sulphoaluminate cement by cut-filling process. The influences of PMN volume fraction and water/cement ratio on the properties of the composite were investigated. The results showed that the d_{33} value increase rapidly with increasing volume fraction of PMN. The water/cement ratio has little influence on piezoelectric properties of 2-2 cement based piezoelectric composite. Huang *et al.* [83] studied dielectric and piezoelectric properties of 2-2 cement based piezoelectric composite in 2008. The piezoelectric ceramic used was lead magnesium niobate (PMN) ceramic. The results indicated that with increasing the PMN volume fraction, both the d_{33} and the ε_r values of the composite increased, while the g_{33} values decreased.

Table 2.8 Designing parameters of receiving piezoelectric composites [12].

Number #	Dimensions of ceramic plate/rod (L×W×H) (mm)	Space between ceramic plate or rod (mm)	Matrix	Connectivity	Volume fraction of piezoelectric ceramic (%)
0	15 x 10 x 8.6	-	-	-	100
1	15 x 1 x 7.5	1	Cement	2-2	53.9
2	15 x 1 x 7.5	1	Cement/polymer	2-2	53.3
3	1 x 1 x 7.6	0.4	Cement	1-3	54.9
4	1 x 1 x 7.4	0.4	Cement/polymer	1-3	54.8

Xu *et al.* [11] studied the electromechanical properties of 2-2 cement based piezoelectric composite. 2-2 type cement based piezoelectric composites were fabricated by dice-and-fill technique in 2009. The influences of PMN ceramic volume fraction on the electromechanical properties of the composite were investigated. The results indicated that the K_p value of the composite was hardly influenced by the PMN volume fraction, which fluctuates between 35% and 37%, while both the K_t and Q_m values exhibited the increasing trend.

In addition, Xu *et al.* [12] also studied the fabrication and properties of piezoelectric composites designed for process monitoring of cement hydration reaction in 2012. The 2-2 and 1-3 types piezoelectric composites were fabricated by cutting and filling technique. The piezoelectric ceramic used was lead zirconate titanate piezoelectric ceramic; PZT. The parameters of the piezoelectric composites were designed, as given in Table 2.8. The results are given in Table 2.9.

Table 2.9 Main properties of the receiving type piezoelectric elements [12].

	0#	1#	2#	3#	4#
d_{33} (pCN^{-1})	600	339	531	240	296
g_{33} ($mVmN^{-1}$)	24.00	24.40	28.20	24.65	32.47
ε_r	22.00	1570	1120	1100	1030
tan δ (%)	2.00	7.50	2.37	4.50	2.5
K_p (%)	62	48.71	49.27	35.72	45.92
K_t (%)	50	59.84	69.20	55.83	68.21
Q_m	80	6.76	3.93	7.6	3.38
Z (M Rayl)	24.7	14.8	6.8	13.2	6.4
f_r-planar (kHz)	77.74	80.96	78.46	85.96	70.97
f_r-thickness (kHz)	327.06	205.90	200.90	190.91	166.25

The research showed that these piezoelectric composites had larger piezoelectric voltage factor, thickness electromechanical coupling coefficient and lower acoustic impedance than the pure piezoelectric ceramic. The 2-2 type piezoelectric composites had higher piezoelectric strain factor, planar and thickness electromechanical coupling coefficients, while 1-3 type piezoelectric composites had higher piezoelectric voltage factor and lower acoustic impedance value.

In 2012, Chaipanich *et al.* [84] studied the dielectric properties of 2-2 connectivity lead magnesium niobate-lead titanate PMT-PT/cement composites. The composites were fabricated using a dice and fill technique and cured in 98%RH curing chamber for 7 days before measurements. Dielectric constant (ε_r) at 1 kHz

increased with PMN-PT of 60-80 % by volume, having values of 1504, 1645 and 2390 respectively. Dielectric loss (*tan δ*) values were 0.382, 0.185 and 0.188 at 1 kHz.